Investigation of metastable states and nucleation in the kinetic Ising model

K. Binder* and H. Müller-Krumbhaar†
IBM Zurich Research Laboratory, 8803 Rüschlikon-ZH, Switzerland
(Received 19 October 1973)

The relaxation of a two-dimensional Ising ferromagnet after a sudden reversal of the applied magnetic field is studied from various points of view, including nucleation theories, computer experiments, and a scaling theory, to provide a description for the metastable states and the kinetics of the magnetization reversal. Metastable states are characterized by a "flatness" property of the relaxation function. The Monte Carlo method is used to simulate the relaxation process for finite $L \times L$ square lattices ($L = 55$, 110, 220 and 440, respectively); no dependence on L is found for these systems in the range of magnetic fields calculated. The metastable states found for small enough fields terminate at a rather well-defined "coercive field," where no singular behavior of the susceptibility can be detected, within the accuracy of the numerical calculation. In order to explain these results an approximate theory of cluster dynamics is derived from the master equation, and Fisher's static-cluster model, generalizing the more conventional nucleation theories. It is shown that the properties of the metastable states (including their lifetimes) derived from this treatment are quite consistent with the numerical data, although the details of the dynamics of cluster distributions are somewhat different. This treatment contradicts the mean-field theory and other extrapolations, predicting the existence of a spinodal curve. In order to elucidate the possible analytic behavior of the coercive field we discuss a generalization of the scaling equation of state, which includes the metastable states in agreement with our data.

I. INTRODUCTION

Since the pioneering work of van der Waals[1] on the equation of state of a dense gas, the question of existence and properties of metastable states associated with first-order phase transitions remains a challenge to the theoretical physicist. Experimentally, these states have been found near the transitions of various systems, e.g., parts of the hysteresis loop associated with the magnetization reversal in a ferromagnet or with phase separation in alloys, supercooled vapor and superheated liquid associated with condensation or evaporation, supercooled liquid associated with crystallization, and many crystallographic phases associated with structural phase transitions. Since the lifetimes of these states are astronomically large in some cases (e.g., diamond), the properties of these states may be very well defined from the experimental point of view. However, in most cases it is an open question how far these states extend into the region of the stable phase, since due to (heterogeneous) nucleation processes it may be experimentally impossible to reach a "spinodal curve" even if it exists.

In contrast to this characterization of experiments the progress of the theory of phase transitions has made the theoretical aspects of metastable states still more obscure. A rigorous reanalysis[2] of van der Waals's treatment exhibited the fact that these states cannot be obtained from the evaluation of a partition function in the thermodynamic limit even in cases where the van der Waals description is correct for the true equilibrium states. The metastable states are obtained in a peculiar limit only[3] where the volume V and the range of interaction are taken to infinity together; in this limit also the lifetime of these states tends to infinity. If the dynamics of systems with infinite long-range forces may be described by a time-dependent Ginzburg-Landau equation, detailed exact descriptions of the relaxation processes associated with the metastable states are available.[4] It is not expected, however, that these results have much relevance to physical systems with short-range forces. At least, Fisher's suggestion that the Ising model exhibits an essential singularity at the coexistence curve [5] indicated that any analytic continuation of the stable states to the metastable states seemed ambiguous. Nevertheless extrapolation techniques[6] indicated the existence of some singularities at a "pseudospinodal"[6,7] also for the Ising model. As a consequence it was suggested by various authors[5,8–10] that a more detailed kinetic investigation of the transition from the metastable to the stable phase should be made.

It is the intention of the present paper to make a contribution to this question, investigating numerically some static and dynamic aspects of metastable states in the single-spin-flip kinetic Ising model.[11–13] In Sec. II we briefly recall the basic ideas about metastability. Contrary to some previous treatments we prefer a dynamic characterization of metastability. We define metastable states by a suitable "flatness" property of a certain nonequilibrium relaxation function. This point of view has been discussed in more detail in a previous

publication[4] and shown to be consistent also with the soluble case of long-range models.

In Sec. III we introduce the model considered. Even in two dimensions, no exact treatments are available to obtain information concerning the dynamics of this model.[13] In order to provide a firm basis for the subsequent discussions, we use the Monte Carlo method[14–22] to obtain numerical results concerning both the nonequilibrium relaxation functions and the detailed time dependence of cluster distributions. The Monte Carlo method provides an exact numerical solution to the basic master equation of the model, but can be applied to systems of finite size only. Using periodic boundary conditions we detected almost no dependence of the results on the size of the system for the range of temperatures and fields considered, in contrast to the preliminary results with free boundaries[19] where "heterogeneous nucleation" takes place at the surface. Our results apply to magnetic fields that are constant in time, which seems more realistic than the calculations with stepwise time-dependent magnetic fields.[20]

In Sec. IV we discuss the question to what extent these "experimental" results of the computer simulation may be understood by suitable approximations to the exact master equation. While a factorization approximation to the kinetic equation for the spin yields the well-known mean-field results[4,12] only, a factorization approximation to the very complicated exact kinetic equation for the cluster distribution yields a generalization of the nucleation theory. It has been shown[23,24] that metastable states and their lifetimes may be discussed on a statistical basis avoiding the very phenomenological nucleation picture. In our derivation we rather try to reconcile this concept with statistical mechanics, elucidating the (admittedly very crude) approximations involved in the derivation of conventional nucleation theory from the exact master equation in this model. The static properties of clusters as described by Fisher's droplet model[5,25–27] are incorporated into our generalized nucleation theory in the same way as in the more phenomenological treatments of Kiang *et al.*[28] and Eggington *et al.*[29] For the sake of completeness we discuss the implications of this static cluster model in the Appendix. Section V contains some conclusions and suggestions for further investigations along these lines. A very brief account on some parts of the present work was given in Ref. 30.

II. BASIC CONCEPTS ABOUT METASTABILITY

A simple scheme to characterize a state as stable, metastable, and unstable has been provided by Gibbs[31] who suggested that also metastable and unstable "states" may be described by a thermodynamic potential G. Equilibrium is characterized by

$$(\delta G)_{eq} = 0 \quad , \tag{1}$$

while stability of a state against perturbations is ensured by

$$(\Delta G)_{eq} > 0 \quad . \tag{2}$$

If for a state Eq. (2) is violated with respect to certain finite perturbations, but still holds for infinitesimal ones,

$$(\delta^2 G)_{eq,MS} > 0 \quad , \tag{3}$$

this state is called metastable. For a more detailed discussion of criteria of this kind see the book by Glansdorff and Prigogine.[32] Choosing as independent variables appropriate to the Ising model, the temperature, and the magnetic field H,[33] Eq. (3) can be brought into a more explicit form

$$\left.\frac{\partial^2 G}{\partial T^2}\right|_H (\delta T)^2 + \left.\frac{\partial^2 G}{\partial H^2}\right|_T (\delta H)^2 + 2\,\frac{\partial^2 G}{\partial H \partial T}(\delta T\,\delta H) > 0 \quad , \tag{4}$$

implying as a necessary condition of stability that both specific heat and susceptibility are positive,

$$C_H > 0, \quad \chi_T > 0 \quad . \tag{5}$$

Note that χ_T diverges as the spinodal curve of the mean-field theory (see Sec. IV A), changing there from $+\infty$ to $-\infty$ in accordance with the above criterion. The distinction between stable and metastable states is more difficult. Furthermore, the existence of a thermodynamic potential outside equilibrium is an open question.[34] While Eqs. (4) and (5) are certainly necessary conditions for stability if G exists, it is not obvious if they are sufficient. The system may well be stable with respect to global variations δT, δH, but unstable with respect to local variations, e.g., the formation of a "critical nucleus" bringing the system from the metastable to the stable equilibrium state. Even if an extrapolation of G beyond the equilibrium states exists, it may perhaps be meaningless already for values of H, T far from the spinodal curve suggested by Eq. (5), if such an instability against local fluctuations becomes important.[5,7] This concept of "critical-nucleus formation" is essentially the basic idea of nucleation theory,[35–44] which will be reformulated for the kinetic Ising model in Sec. IV.

Assuming that an extrapolation of the potential G from the stable to the metastable states exists, it is not yet clear how to construct it explicitly. Equilibrium statistical mechanics yield information about true equilibrium states only, if the partition function is evaluated correctly, as shown from the rigorous treatment of the van der Waals gas.[2] Langer[8] suggests the construction of G by analytic continuation of the droplet-model equation

of state; since the droplet model has an essential singularity at $H=0$ and this analytic continuation is complex, its imaginary part may be taken as a measure of the lifetime of the metastable state. This latter conjecture is substantiated[6,23,24] by more general dynamic considerations.

Another possibility of extrapolation beyond the equilibrium state is provided by the application of the series extrapolation techniques.[6,45,46] These techniques were unable to give any indication of an essential singularity at the coexistence curve. Padé approximants at fixed magnetization were consistent with the existence of a spinodal curve, where the susceptibility diverges. While the exponent of this curve was found equal to the order parameter, the difference of its critical amplitudes was too small to be determined accurately by this method in two dimensions. This fact implies that the "pseudospinodal curve"[7] located by the technique is extremely close to the phase boundary in two dimensions. Only rather inaccurate information on the location of the coercive fields is available. While these authors expressed serious doubts on the existence of an essential singularity at the coexistence curve, the discussion of Domb[10] supports the existence of such a singularity, referring to a rigorous theorem of Lanford and Ruelle.[47] Since this singularity (if it exists!) seems to be very weak (according to the cluster model all derivatives of the free energy are finite in the limit $H \to 0^+$ for $T < T_c$), it is not detected by numerical work or experiments,[7] where a similar extrapolation to a "pseudospinodal curve" was readily feasible. Chu *et al.*[7] stressed the fact that true information on the metastable state itself cannot be found by such extrapolations.

Emphasizing the point that these purely static techniques are not sufficient to give precise information on metastable states, considerations of the dynamic behavior are needed. First we mention the kinetic theory of stability[32]; this method separates the unstable from stable and metastable states considering their normal modes. If modes occur whose frequencies have a negative imaginary part, i.e., lead to an increase of fluctuations with time, the state is called unstable. In this technique it is again supposed that the thermodynamic potential is known explicitly (one expands the potential by a quadratic form in the appropriate displacements characterizing the fluctuations and determines the corresponding eigenvalues). In practice, it is restricted to mean-field approximations, e.g., the theory of spinodal decomposition.[48,49]

Perhaps the most interesting definition is provided by the recent important work of Penrose and Lebowitz[3] in their investigation of the metastable states of the van der Waals gas. These authors call a state metastable if (i) only one thermodynamic phase is present; (ii) a system that starts in this state is likely to take a long time to get out; and (iii) once the system has got out, it is unlikely to return. The meaning of "long time to get out" is made precise by these authors introducing an arbitrary subdivision of the system into cells, and considering the density fluctuations among these cells by means of classical mechanics (for details see Ref. 3). Since their techniques rest heavily on the consideration of a long-ranged potential, extensions to other systems are far from straightforward.

In the following we will adopt another point of view, which seems appropriate both with respect to formal requirements and to heuristic arguments originating from the evaluation of numerical data. This approach starts from the experimental procedure, where some nonequilibrium relaxation process is considered: If in the course of this process a "state" occurs whose evolution in time is negligibly small for times which are large compared to the equilibrium relaxation times of the system, this state is taken as a metastable state.

A precise description of such a nonequilibrium relaxation process may be obtained as follows. We describe the system considered in terms of dynamical coordinates $\{\mu_i(t)\}$ [e.g., in the kinetic Ising model, $\mu_i(t)$ is the magnetic moment of the particle at lattice site i]. Introducing the density matrix $\rho^{\mu}_{T,H'}$ characterizing thermal equilibrium in the state T, H' the expectation value of an operator A_μ is given by

$$\langle A_\mu \rangle_{T,H'} \equiv \mathrm{Tr}\, \rho^{\mu}_{T,H'} A_\mu = \frac{\mathrm{Tr}\, e^{-\mathcal{H}/k_B T} A_\mu}{\mathrm{Tr}\, e^{-\mathcal{H}/k_B T}} \quad , \tag{6}$$

where $\mathcal{H}$ is the Hamiltonian of the system.

From Eq. (6) and the definition of a Liouvillean $\mathfrak{L}$,

$$\mu_i(t) = e^{-i\mathfrak{L}t}\, \mu_i(0) \quad , \tag{7}$$

the Born-Bogoliubov-Green-Kirkwood-Yvon (BBGKY) hierarchy[50] for the correlation function is derived:

$$\frac{d}{dt} \langle \mu_i(t) \rangle_{T,H'} = -i \langle \mathfrak{L} \mu_i(t) \rangle_{T,H'} \quad ,$$

$$\frac{d}{dt} \langle \mu_i(t)\, \mu_j(t) \rangle_{T,H'}$$

$$= -i \langle [\mathfrak{L} \mu_i(t)]\, \mu_j(t) \rangle_{T,H'} - i \langle \mu_i(t) [\mathfrak{L} \mu_j(t)] \rangle_{T,H'} \quad , \tag{8}$$

etc. This description is appropriate both for equilibrium and nonequilibrium processes. Consider a case where the system was in thermal equilibrium for times $t < 0$ at T and H',[51] and at $t = 0$ these external variables are changed suddenly by ΔT_l, ΔH_l.[52] To lowest order the subsequent nonequilib-

rium relaxation process may be characterized by a "nonequilibrium relaxation function" [4,53]

$$\phi_\mu^{\Delta H_I,\Delta T_I}(\vec{k},t)\equiv\sum_{r_i}e^{i\vec{k}\cdot\vec{r}_i}\left[\langle\mu_i(t)\rangle_{T,H'}-\langle\mu_i(\infty)\rangle_{T,H'}\right]\Big/ \sum_{r_i}e^{i\vec{k}\cdot\vec{r}_i}\left[\langle\mu_i(0)\rangle_{T,H'}-\langle\mu_i(\infty)\rangle_{T,H'}\right] \quad . \tag{9}$$

Note that the expectation values are taken in the ensemble of the initial state, while the $\mathcal{L}$, appropriate to the final state T_I, H_I,

$$T=T+\Delta T_I,\quad H_I=H'+\Delta H_I\ , \tag{10}$$

has to be taken in Eq. (9). In ergodic systems where

$$\langle\mu_i(\infty)\rangle_{T,H'}=\langle\mu_i\rangle_{T_I,H_I}\quad , \tag{11}$$

equation (9) reduces to familiar time-dependent pair correlations in the limit ΔH_I, $\Delta T_I\to 0$. [4,22] While $\phi_\mu^{\Delta H_I,\Delta T_I}(\vec{k},t)$ can be calculated by direct integration of Eq. (8) only in exceptional cases (e.g., the time-dependent Ginzburg-Landau theory[4]), it will become apparent in later sections that both the computer experiment technique and the nucleation theory yield readily $\phi_\mu^{\Delta H,0}(0,t)\equiv\phi(t)$.

As an example we show $\phi(t)$ as obtained from the mean-field approximation (MFA) [see Sec. IV A] in Fig. 1. Curves for magnetic fields exceeding the coercive field H_s^* are given [for notation see Sec. III B]. It is seen that for H_s near H_s^* a very flat portion in the relaxation curve develops, announcing the occurrence of metastable states. While in the MFA their lifetime is infinite, finite lifetimes will be observed in models with short-range interactions; in this case the relaxation curve will always look qualitatively similar to the flat curves of Fig. 1. We define the relaxation time τ_R of the process by

$$\tau_R=\int_0^\infty\phi(t)\,dt\quad . \tag{12}$$

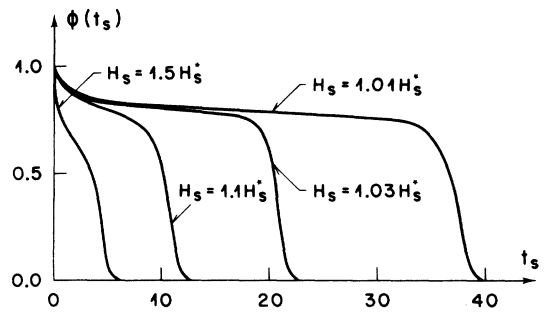

FIG. 1. Nonequilibrium relaxation function $\phi(t_s)$ plotted vs the scaled time [Eq. (30)], as obtained from the time-dependent Ginzburg-Landau theory. Curves for various values of the scaled field H_S [Eq. (29)] are shown.

It is then appealing to define the order parameter μ^{MS} of the metastable state, within a given inaccuracy $\delta\mu$, as a time average over the flat part of the relaxation curve

$$\mu^{MS}=\mu_{t_1t_2}\equiv\frac{1}{t_2-t_1}\int_{t_1}^{t_2}\phi(t)\,dt\quad , \tag{13}$$

where "flatness" implies that times $t_I\ll\tau_R$ and t_F can be found, such that for all times t_1, t_1', and t_2, the subsequent inequalities are fulfilled, [4]

$$t_I\le t_1\le t_1'<t_2<t_F\quad , \tag{14}$$

$$\mu_{t_1t_2}-\mu_{t_1't_2}<\delta\mu\ll\mu_{t_1t_2}\quad , \tag{15}$$

$$\delta\mu/\delta\mu_R\ll(t_F-t_I)/\tau_R\quad ,$$

where $\delta\mu_R\equiv\min\{\mu_{t_1t_2}-\langle\mu\rangle_{T,H'+\Delta H}\}$. We may denote τ_R' as a lifetime of the metastable state

$$\tau_R'=\tau_R\left(\langle\mu(0)\rangle_{T,H'}-\langle\mu(\infty)\rangle_{T,H'}\right)/\left(\mu^{MS}-\langle\mu(\infty)\rangle_{T,H'}\right)\quad . \tag{16}$$

For a more detailed discussion of this flatness criterion see Ref. 4. Here we only note that this definition is sufficiently general, so that it does not prejudice the question of the existence of thermodynamic potentials, etc. Lack of safe knowledge about metastability leads us to use this "constructive definition" of metastable states Eqs. (13)–(16) as a working hypothesis in the following sections. In fact, it may be consistent with any of the definitions previously mentioned. We think Eqs. (13)–(16) to be necessary conditions for a metastable state, but they might not be sufficient.

III. KINETIC ISING MODEL AND MONTE CARLO METHOD

A. General theory

In the single-spin-flip kinetic Ising model introduced by Glauber[11] an assembly of Ising spins is considered, which are in contact with a heat bath. This bath induces random flips of the spin from one state to another, in accordance with prescribed transition probabilities $W(\mu_i\to-\mu_i)$. Since only one spin is permitted to flip at once, neither the order parameter nor the energy are conserved quantities. Since W is assumed to depend on the actual state of the system only, independent of the "history" of the system, the dynamics of the system is governed by a Markovian master equation for the probability distribution $P(\mu_1,\ldots,\mu_N,t)$[11,12]:

$$\frac{d}{dt}P(\mu_1,\ldots,\mu_N,t)=-\sum_{j=1}^{N}W(\mu_j\to-\mu_j)\,P(\mu_1,\ldots,\mu_j,\ldots,\mu_N,t)$$

$$+\sum_{j=1}^{N} W(-\mu_j \to \mu_j) P(\mu_1, \ldots, -\mu_j, \ldots, \mu_N, t) \quad . \tag{17}$$

The thermal equilibrium distribution $P_0(\mu_1, \ldots, \mu_N)$ is the stationary state of this equation because of the detailed-balance condition for W:

$$W(\mu_j \to -\mu_j) P_0(\mu_1, \ldots, \mu_j, \ldots, \mu_N) = W(-\mu_j \to \mu_j) P_0(\mu_1, \ldots, -\mu_j, \ldots, \mu_N) \quad . \tag{18}$$

Of course this condition does not specify W uniquely. Two simple choices for W satisfying Eq. (18) are

$$W(\mu_j \to -\mu_j) = (1/2\tau_s)(1 - \mu_j \tanh E_j/k_B T) \quad , \tag{19}$$

$$W'(\mu_j \to -\mu_j) = \begin{cases} (1/\tau_s) e^{-2\mu_j E_j / k_B T} , & \mu_j E_j > 0 \\ (1/\tau_s) & \text{otherwise} , \end{cases} \tag{20}$$

where $\mu_j E_j$ is the energy of the jth magnetic moment,

$$E_j = \mu_B H' + \sum_k J_{jk} \mu_k, \quad \mathcal{H}^{\text{Ising}} = -\sum_j \mu_j E_j \quad . \tag{21}$$

The arbitrary single-spin-flip time τ_s fixes the time scale. The time-dependent expectation value $\langle \mu_j(t) \rangle$ is given by[12]

$$\langle \mu_j(t) \rangle = \sum_{\{\mu\}} \mu_j P(\mu_1, \ldots, \mu_N, t) \quad , \tag{22}$$

where the sum is taken over all possible configurations. From Eqs. (17)–(22) one derives precisely the equation of motion [Eq. (8)]; noting that in this case $\mathfrak{L} \equiv iL$ is given by[54]

$$L = \sum_{j=1}^{N} W_j(\mu_j \to -\mu_j)(1 - P_j) \quad , \tag{23}$$

P_j being the spin-flip operator of the jth spin,

$$P_j \mu_k = -\mu_k \delta_{jk} + \mu_k (1 - \delta_{jk}) \quad . \tag{24}$$

While in the limit where the interactions J_{ij} get long ranged it is shown that different choices of W always lead to the same type of equations of motion in the critical region, where only τ_s is renormalized,[18] the effect of different W's on the detailed dynamics of short-range models can be accounted for in this way only (if at all) near thermal equilibrium.[22] To investigate the influence of the choice for W we shall use both possibilities [Eqs. (19) and (20)] in the numerical investigation.

Nonequilibrium relaxation processes can be treated without approximations only in a rather special case, namely, for the choice Eq. (19) and one-dimensional systems.[55] This case is of no particular interest for us, since there is no spontaneous magnetization and hence one observes no metastable states associated with a first-order transition from positive to negative magnetic fields.

A possibility to solve Eq. (17) for high-dimensional systems is established by the Monte Carlo method.[17,18,22] Here explicit spin configurations $\{\mu_1, \ldots, \mu_N\}$ are generated on the computer with the help of random numbers. While this method is exact in principle, it is restricted to systems of rather small size (the largest N investigated so far is provided by the data of the $N = 440 \times 440$ system described in the present paper) and to limited accuracy due to technical reasons.[18]

The details of the Monte Carlo procedure are as follows. One starts with an initial spin configuration (usually the completely ordered ferromagnet), selects a spin j at random and determines $W(\mu_j \to -\mu_j)$. This spin is flipped if $\tau_s W(\mu_j \to -\mu_j)$ exceeds a random number between 0 and 1. If the spin is not flipped the old configuration is counted as a new configuration. This process is repeated many times. Thus a sequence of new spin configurations is generated, where the number of configurations corresponds to the time lapse. It is convenient to use as a time unit the number of Monte Carlo steps (MCS) divided by the number of spins (N), i.e., the time in which, on the average, any spin has the possibility to flip once. This time unit is independent of the number of spins N. The system now relaxes to the thermal equilibrium appropriate to the chosen external variables ($H' > 0, T$). These configurations, characteristic for this equilibrium state, are then chosen as initial configurations for runs to simulate the nonequilibrium relaxation process under consideration; i.e., after some time the time scale is put to zero, the external variables are put to ($H' + \Delta H \equiv H < 0, T$) and the Monte Carlo process is continued. Both the full information contained in the spin configurations and average quantities like $\tilde{\mu}^{(m)}(t)$:

$$\tilde{\mu}^{(m)}(t) = \frac{1}{N} \sum_{j=1}^{N} \mu_j^{(m)}(t) = \frac{1}{N} \sum_{j=1}^{N} \mu_j^{(m)}\left(\frac{k}{N}\right) \quad , \tag{25}$$

are readily available at every "instant of time" (e.g., at the kth configuration of the Markov chain).[17,21] In order to have better statistics a further average over several independent runs m was taken,

$$\overline{\mu}(t) = \frac{1}{M} \sum_{m=1}^{M} \tilde{\mu}^{(m)}(t) \quad , \tag{26}$$

and this average was taken as an estimate for $\langle \mu(t) \rangle_{T,H}$, necessary to calculate the nonequilibrium relaxation function.

While this Monte Carlo technique has been used extensively for the computation of static equilibrium properties,[14–22,56] applications to dynamic problems did not appear until quite recently.[17–22] More detailed descriptions of the technique and justifications for the accuracy, are contained in Refs. 18 and 22, where the critical slowing down of the kinetic Ising model was investigated. The

nonequilibrium relaxation (where the system is heated suddenly from zero to T, or—equivalently—an infinite field was turned off) was first considered by Ogita *et al.*,[17] while the nonequilibrium relaxation after a sudden reversal of the field was investigated in Ref. 19 in the case of free boundaries. In this case a pronounced dependence on N was detected, because of the enhanced probability of nucleation at the surface of a small metastable system. In Sec. III B we give an analysis of the nonequilibrium relaxation process in the case of periodic boundary conditions.[57]

B. Results for periodic square lattices with nearest-neighbor interactions

Calculations have been performed for $L \times L$ lattices in the range $L = 55$, 110, 220, and 440, at temperatures $J/k_BT = 0.45$, 0.46, and 0.48 (the critical temperature is $J/k_BT_c \approx 0.4407$)[58]; although $\langle \mu \rangle_{T,0} \equiv 0$ for finite systems we were able to work with $\mu_B H'/k_BT = 0$ as the initial state, since at the temperatures considered the systems were perfectly metastable with nonzero magnetization, which agreed with the exact solution[59] within the statistical error. For a discussion of these equilibrium properties in the two-dimensional Ising model as deduced by Monte Carlo methods, see Refs. 19, 22, 60, and 61. A typical equilibrium spin configuration, as used as initial configuration for the magnetization reversal process, is shown in Fig. 2 for $L = 55$ at $J/k_BT = 0.48$. Reversed spins from small clusters are distributed on a background of up spins; the mean magnetization of this configuration is close to the theoretical value $\langle \mu \rangle_{T,H'} = 0.8775$. By "cluster" one denotes a group of reversed spins linked together by nearest-neighbor interactions. Denoting the average concentration of clusters containing l spins at time t by $n_l'(t)$ the time-dependent average magnetization is written

$$\langle \mu(t) \rangle_{T,H'} = 1 - 2 \sum_{l=1}^{N} l n_l'(t) \quad . \tag{27}$$

The cluster distribution in thermal equilibrium was investigated in Refs. 60 and 61 and shown to be consistent with Fisher's cluster model.[5] Since Eq. (27) and the dynamic evolution of the cluster distribution may provide the key to understanding the magnetization-reversal process, as pointed out in Sec. IV B, we give a short description of the cluster model in the Appendix, together with some further simulation results.

Let us first study the magnetization-reversal process at high magnetic fields (i.e., fields considerably exceeding the coercive field), see Fig. 3. A "short" time after this field has been

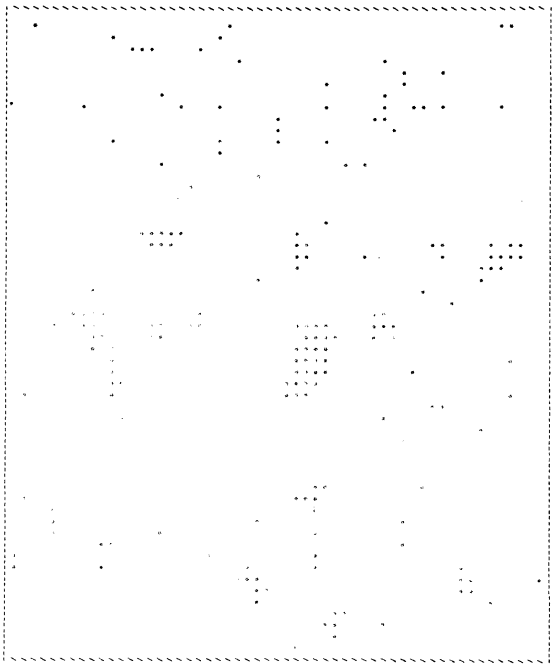

FIG. 2. Spin configuration of the 55×55 square lattice obtained in the thermal-equilibrium state at $J/k_BT = 0.48$. Lattice sites with spin down are characterized by the symbol *, while lattice sites with spin up are left white. All numerical calculations refer to the case $H' = 0$.

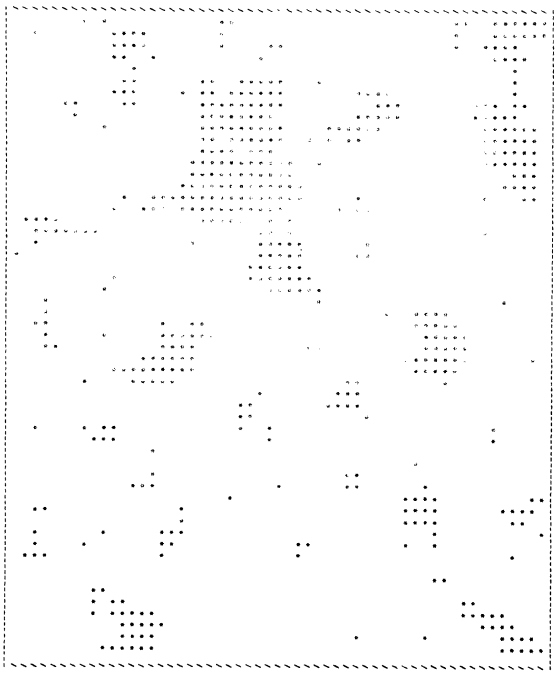

FIG. 3. Spin configuration of the 55×55 square lattice at $J/k_BT = 0.48$, at $t = 95$ MCS per spin after a field $\mu_B H/k_BT = -0.07$ has been switched on (cf. Fig. 2 for further explanations).

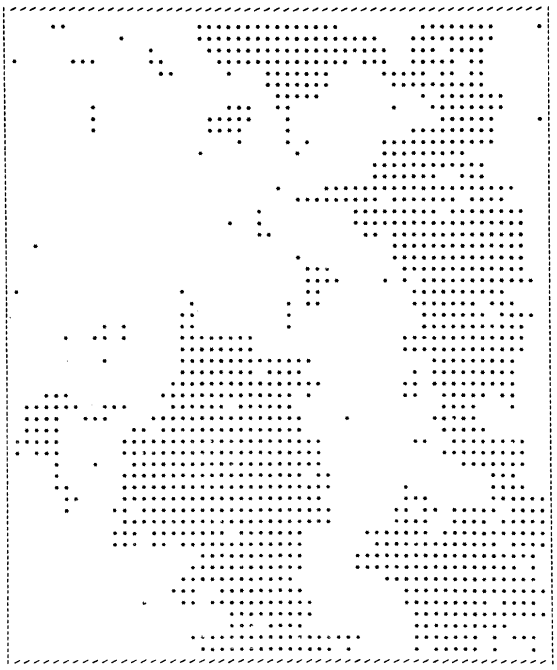

FIG. 4. Spin configuration of the 55×55 square lattice at $J/k_BT = 0.48$, at $t = 145$ MCS/spin after a field $\mu_B H/k_BT = -0.07$ has been switched on (cf. Fig. 2 for further explanations).

switched on ($t = 95$, the equilibrium relaxation time of the order parameter at this temperature is $\tau^{-}_{\delta\mu\delta\mu} \cong 20$) relatively large clusters occur. While the very small clusters which also occur in equilibrium coalesce and disintegrate again, the larger clusters are rather stable and grow by incorporation of smaller clusters in their evnironment. It seems that there exists a "critical size" preventing the clusters from dissociation. Finally (Fig. 4, $t = 145$), very large clusters grow together, forming a macroscopic "cluster" of the new spin-down phase. Within this phase, clusters of the old phase are seen, which shrink steadily in the further course of the process until the state of the system looks like a negative of Fig. 2. In Ref. 21 (and the associate movie picture) a far more detailed description is given for $L = 220$.

This behavior of the clusters may be understood as a competition between the two energies involved in the Hamiltonian [Eq. (21)], the Zeeman energy ($\propto H$), and the exchange energy ($\propto J$). To form a cluster from the bulk costs exchange energy mainly at its surface, while it costs Zeeman energy also within the "bulk" of the cluster. If $H < 0$, however, the Zeeman energy favors the formation of clusters, in contrast to the exchange energy. For small clusters and small $|\mu_B H/J|$ the "surface energy" of the clusters still exceeds their "bulk energy," these clusters are thermodynamically unstable. Although they are built up by thermal fluctuations they will, on the average, disintegrate again. There exists a critical size, however, where the loss by surface energy is compensated for by a gain in bulk energy: Clusters larger than this size are already stable with respect to dissociation; on the average they will thus grow as long as enough up spins in their environment are available. It is evident from Fig. 4 that inside these large clusters the local equilibrium corresponding to the new phase is already established. The point of view adopted here is precisely the idea of the conventional nucleation theory[35–41]; it is seen that this concept receives qualitative support from the computer experiment. In Sec. IV B we shall make the arguments sketched above more quantitative, deriving a theory of cluster dynamics from the master equation which contains the conventional nucleation theory as a special case. In order to apply the ideas discussed in Sec. II we have to calculate the nonequilibrium relaxation functions: These functions are shown for $L = 110$, $J/k_BT = 0.45$, 0.46, and 0.48 in Figs. 5–7, respectively. Parameter of the curves is the magnetic field $-\mu_B H/k_BT$. At large values of $-\mu_B H/k_BT$ the slope of the $\phi(t)$ curve increases with time in the early stages of the magnetization-reversal process. In the later stages of the process $\phi(t)$ relaxes like $e^{-(\text{const})\times t}$. However, for intermediate values of $-\mu_B H/k_BT$ the slope of the $\phi(t)$ curve decreases with time at the beginning of the reversal process. It is seen that a rather flat portion in this curve develops, a precursor of an unstable state. For small values of $-\mu_B H/k_BT$ this metastable state can be clearly recognized from the $\phi(t)$ function. The magnetization relaxes rather quickly (i.e., exponentially) towards this meta-

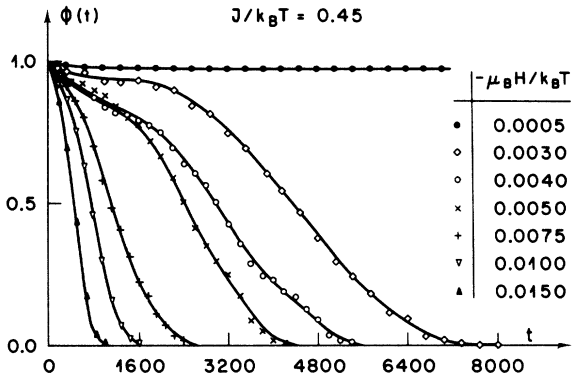

FIG. 5. Nonequilibrium relaxation functions $\phi(t)$ plotted vs time (in Monte Carlo steps per spin) at $J/k_BT = 0.45$ for various values of $\mu_B H/k_BT$. This calculation was performed with the transition probability Eq. (19), and $H' = 0$.

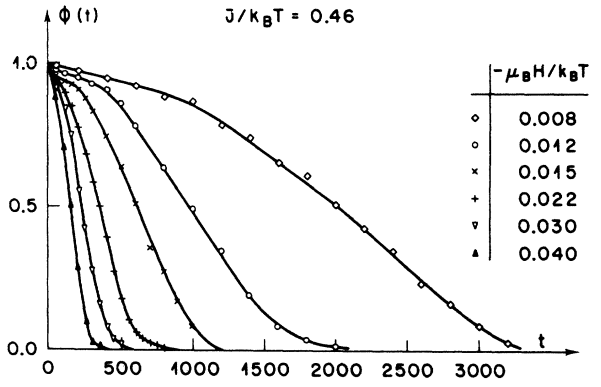

FIG. 6. Nonequilibrium relaxation functions $\phi(t)$ plotted vs time at $J/k_BT = 0.46$ for various values of μ_BH/k_BT and $H' = 0$.

stable state, and its lifetime is so large that it is not possible to investigate it by the computer experiment. If this metastable "state" has any residual time dependence, it is by far smaller than the statistical error of this numerical calculation.

It is interesting to associate the various stages of the nucleation process as demonstrated from the "raw-data" configuration pictures (Figs. 2–4) with the various parts of the nonequilibrium relaxation function. During the first (concave) part of $\phi(t)$ small clusters typical for thermal equilibrium are present, and their concentration increases to values typical for the metastable state. In this state (flat region) small clusters grow together to form clusters of intermediate size; these intermediate clusters are sufficiently rare so that they do not interact, and in most cases they disintegrate again. After long enough time, however, clusters have originated by such fluctuations which are already comparatively stable against dissociation. By incorporation of intermediate clusters these clusters grow rather quickly and this region corresponds to the linear decrease of $\phi(t)$ with time. While the thermal equilibrium state may be characterized as a weakly interacting gas of clusters,[62] we have many cluster-to-cluster interactions in this region. Here the large clusters form a coherent background of spin-down phase and the remainder of spin-up phase has now to be considered as clusters in this new phase. Their steady disappearance corresponds to the last exponential part of $\phi(t)$.

Considering now the temperature dependence of the $\phi(t)$ function it is to be noted that Figs. 5–7 look rather similar, apart from irregularities due to poor statistics. This qualitative statement can be made more precise extending the dynamic scaling hypothesis (DSH)[63,64] to nonequilibrium phenomena,[30] i.e., we require

$$\phi_\mu^{\Delta H}(\vec{k}, t) \equiv G(\epsilon, H, H', \vec{k}, t) = G_S(H_S, H_S', \vec{k}_S, t_S) \quad , \tag{28}$$

where we introduced the scaled variables ($\epsilon = 1 - T/T_c$)

$$H_S = H\epsilon^{-\beta\delta}, \quad H_S' = H'\epsilon^{-\beta\delta} \tag{29}$$

and

$$\vec{k}_S = \vec{k}\epsilon^{-\nu}, \quad t_S = t\epsilon^{+\Delta_{\delta\mu\delta\mu}} \quad . \tag{30}$$

By β, δ, and ν we denote the standard critical exponents, and by $\Delta_{\delta\mu\delta\mu}$ the critical exponent of the order-parameter correlation function $\phi_{\delta\mu\delta\mu}(0, t)$,[13,22,54]

$$\phi_{\delta\mu\delta\mu}(\vec{k}, t) = \sum_j e^{i\vec{k}\cdot(\vec{r}_j - \vec{r}_i)} \langle \delta\mu_i(0)\, \delta\mu_j(t) \rangle \times \left(\sum_j e^{i\vec{k}\cdot(\vec{r}_j - \vec{r}_i)} \langle \delta\mu_i(0)\, \delta\mu_j(0) \rangle \right)^{-1} ,$$

$$\delta\mu_i = \mu_i - \langle \mu \rangle , \tag{31}$$

$$\tau_{\delta\mu\delta\mu} \sim |\epsilon|^{-\Delta_{\delta\mu\delta\mu}}, \quad \epsilon \to 0 \tag{32}$$

where

$$\tau_{\delta\mu\delta\mu} = \int_0^\infty \phi_{\delta\mu\delta\mu}(0, t)\, dt \quad . \tag{33}$$

We note that Eq. (28) holds in special cases, e.g., the mean-field theory[4] (see Sec. IV A), and in the limit $\Delta H \to 0$ it reduces to the conventional DSH since[4,22]

$$\lim_{\Delta H \to 0} \phi_\mu^{\Delta H}(\vec{k}, t) = \phi_{\delta\mu\delta\mu}(\vec{k}, t) \quad . \tag{34}$$

The DSH seems well established with respect to the two-dimensional kinetic-Ising-model equilibrium relaxation function $\phi_{\delta\mu\delta\mu}(\vec{k}, t)$.[22,65] As a test of the hypothesis, Eq. (28) in our case, we plot in Fig. 8, some functions $\phi(t)$ belonging to (roughly) the same values of the scaled field H_S versus the scaled time. Within some small scatter of data

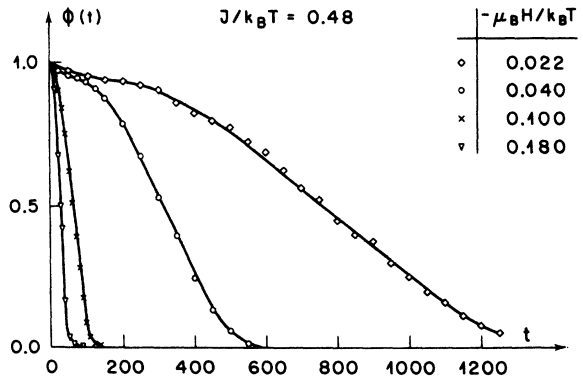

FIG. 7. Nonequilibrium relaxation functions $\phi(t)$ plotted vs time at $J/k_BT = 0.48$ for various values of μ_BH/k_BT, and $H' = 0$.

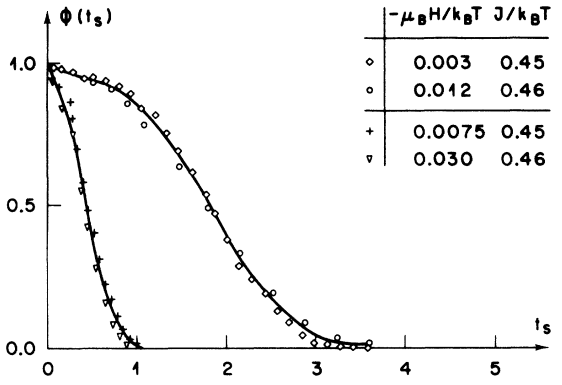

FIG. 8. Nonequilibrium functions $\phi(t_s)$ plotted vs scaled time [Eq. (30)] for two pairs of J/k_BT, μ_BH/k_BT which lead to the same value of the scaled field H_S [Eq. (29)].

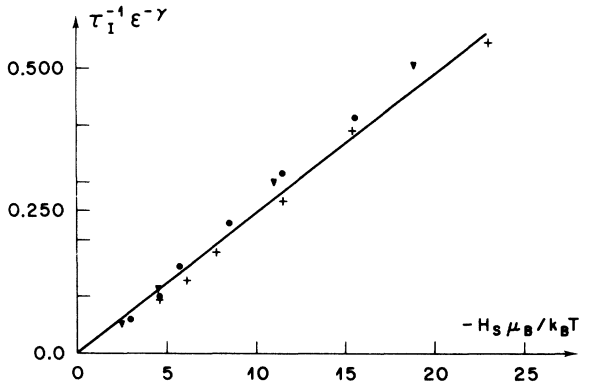

FIG. 10. Scaled initial slope of the nonequilibrium relaxation function plotted vs the scaled field for various temperatures.

points due to statistical inaccuracy scaling behavior is indeed observed. It should be noted that Eq. (28) implies also static scaling for the metastable states, as suggested previously.[6,7,28,30]

Furthermore, it is important to investigate the dependence on the size of the systems used. This is done in Fig. 9 where $\phi(t)$ is plotted versus t at $\mu_BH/k_BT = 0.015$ and $J/k_BT = 0.46$ for various N. No dependence on N was found. We cannot exclude that there is a dependence on N for H near the "coercive field," however, where very longlived metastable states develop. Due to the immense amount of computing time necessary to investigate this problem we made no systematic study of the N dependence.

In Fig. 10 we plot the inverse initial slope of the $\phi(t)$ functions at $t = 0$ versus the scaled magnetic field. The initial decay time τ_I is normalized with ϵ^{γ}, as in the case of equilibrium relaxation functions[22] (see also Sec. IV A). Although these data are not very accurate it is seen that

$$\epsilon^{-\gamma}\tau_I^{-1} = (\text{const}) \cdot H_S \quad , \tag{35}$$

as expected from a Taylor series expansion of $\phi_\mu^{\Delta H}(\vec{k}, t)$ in powers of L [Eq. (23)],

$$\langle \mu(t) \rangle_{T,H'} \cong \langle \mu(0) \rangle_{T,H'} - \langle L\mu(0) \rangle_{T,H'} t - \cdots \, , \tag{36}$$

where one uses

$$\langle L\mu \rangle_{T,H'} = -\langle \mu \rangle_{T,H'} + \left\langle \tanh\left[\left(\mu_B H' + \mu_B \Delta H + \sum_k J_{jk}\mu_k\right)\Big/ k_BT\right]\right\rangle_{T,H'} \, . \tag{37}$$

Expansion in powers of ΔH and use of the steady-state condition

$$\langle \mu \rangle_{T,H'} = \left\langle \tanh\left[\left(\mu_B H' + \sum_k J_{jk}\mu_k\right)\Big/ k_BT\right]\right\rangle_{T,H'} \tag{38}$$

yields

$$\langle L\mu \rangle_{T,H'} \approx \frac{\mu_B \Delta H}{k_BT}\left\{1 - \left\langle \tanh^2\left[\left(\mu_B H' + \sum_k J_{jk}\mu_k\right)\Big/ k_BT\right]\right\rangle_{T,H'}\right\} \, , \tag{39}$$

which is finite at T_c. Thus we immediately get the desired result

$$\tau_I^{-1} \approx \frac{\mu_B \Delta H}{k_BT}\left\{1 - \left\langle \tanh^2\left[\left(\mu_B H' + \sum_k J_{jk}\mu\right)\Big/ k_BT\right]\right\rangle\right\} \times (\langle \mu \rangle_{T,H'} - \langle \mu \rangle_{T,H})^{-1} \tag{40}$$

which has the scaling properties of Eq. (35). Then we investigate the relaxation time τ_R [Eq. (12)], plotting the scaled inverse relaxation time $(\tau_R^S)^{-1}$ for Eq. (19),

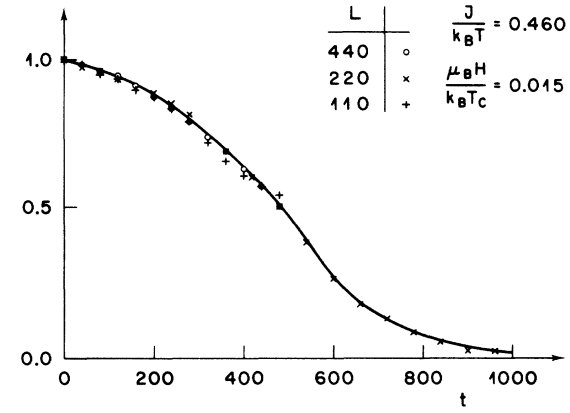

FIG. 9. Nonequilibrium relaxation function $\phi(t)$ plotted vs time at $J/k_BT = 0.46$, $\mu_BH/k_BT = -0.015$ for various values of N. This calculation was performed with the transition probability [Eq. (20)].

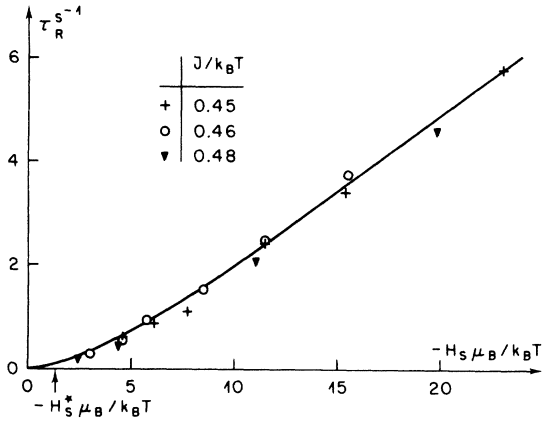

FIG. 11. Scaled inverse relaxation time $(\tau_R^S)^{-1}$ plotted vs the scaled field for various temperatures. The curve represents Eq. (81).

$$(\tau_R^S)^{-1} = \tau_R^{-1}\epsilon^{-\Delta_{\delta\mu\delta\mu}} \tag{41}$$

versus the scaled field H_S in Fig. 11. Again all data points fall on a single curve, as required by the DSH [Eq. (28)]. But while $\tau_I^{-1} \sim H_S$ we observe that the $(\tau_R^S)^{-1}$ curve is extremely flat for $H_S \to 0$, where longliving metastable states occur. The dotted curve shown in the figure is a simple nucleation prediction [Eq. (81), Sec. IV B]. Nucleation theory does not predict any sharp limit of metastability, in contrast to series expansions[6] or scaling estimates (Sec. V). We include the linear model prediction for the coercive field [Eq. (103)]. In this regime of fields well-defined metastable states are found. The data points for the choice Eq. (20)[21] could also be fitted by Eq. (81) with a somewhat different time-scale factor.

In Fig. 12 we compare the magnetic field-dependence of the static fluctuation

$$\chi \equiv (k_BT)^{-1}\,(\langle\mu^2\rangle - \langle\mu\rangle^2) \tag{42}$$

and the order-parameter relaxation time $\tau_{\delta\mu\delta\mu}$ [Eq. (33)] of the metastable states for $J/k_BT = 0.46$. Again the position of the coercive field predicted by Ref. 6 and by Eq. (103) are shown. The curves do not exhibit any singular behavior at these points; if singularities occur their effect is numerically small,[6] however, and might well be overlooked in such numerical investigations. Note that the thermodynamic relation $\chi = \partial\langle\mu\rangle/\partial H$ holds for the metastable states as expected[3,4] (at least within the given accuracy).

In order to provide a more detailed description of metastability and nucleation, it might seem appropriate to investigate the k dependence of $\phi_\mu^{\Delta H}(\vec{k}, t)$. Due to the absence of analytical theories we did not try this, however, and preferred to calculate the time dependence of cluster distributions. As an example the concentration $n_l(t)$ of clusters with l reversed spins are plotted for several times in Fig. 13. Various values of t are shown. The concentrations are normalized by the factor l^τ occurring in the Fisher cluster model [see the Appendix]. It is seen that $n_l(t)$ rather quickly reaches a very flat maximum for small l, and then de-

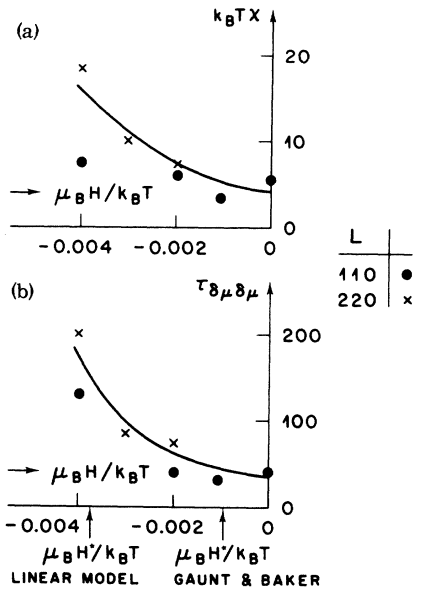

FIG. 12. Static fluctuation of the magnetization "$k_BT\chi$" (a) and order parameter relaxation time $\tau_{\delta\mu\delta\mu}$ (b) of metastable states plotted vs the magnetic field at $J/k_BT = 0.46$ for two values of N. The values H^* are also shown where the series extrapolation (Ref. 6) and the linear model, respectively, predict a singular behavior.

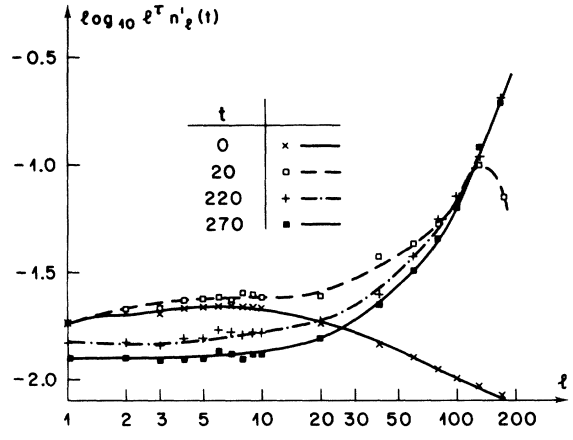

FIG. 13. Normalized cluster distribution $l^\tau n_l'(t)$ plotted double logarithmically vs l at various times at $J/k_BT = 0.46$ and $\mu_BH/k_BT = 0.022$. The relaxation time is in this case $\tau_R \approx 368$ MCS per spin.

creases slowly. A more detailed discussion is postponed to Sec. IV C, where a comparison with nucleation theory is given.

IV. APPROXIMATE THEORIES

A. Mean-field approximation (MFA)

From Eqs. (17) and (23) it is easy to derive the explicit form of Eq. (8), using the relation for the square lattice[54] ($H'=0$),

$$\tanh\left(J\sum_{k(\neq j)}\mu_k\Big/k_BT\right)=\frac{1}{8}\left(\tanh\frac{4J}{k_BT}+2\tanh\frac{2J}{k_BT}\right)\times\sum_{k(\neq j)}\mu_k+\frac{1}{8}\left(\tanh\frac{4J}{k_BT}-2\tanh\frac{2J}{k_BT}\right)\times\sum_{k_1\neq k_2\neq k_3(\neq j)}\mu_{k_1}\mu_{k_2}\mu_{k_3}\quad,\tag{43}$$

which leads to

$$\tau_S\frac{d}{dt}\langle\mu_j(t)\rangle=-\langle\mu_j(t)\rangle+\frac{1}{8}\left(\tanh\frac{4J}{k_BT}+2\tanh\frac{2J}{k_BT}\right)\times\sum_{k(\neq j)}\langle\mu_k(t)\rangle+\frac{1}{8}\left(\tanh\frac{4J}{k_BT}-2\tanh\frac{2J}{k_BT}\right)\times\sum_{k_1\neq k_2\neq k_3(\neq j)}\langle\mu_{k_1}(t)\,\mu_{k_2}(t)\,\mu_{k_3}(t)\rangle\quad.\tag{44}$$

Note that the sums in Eqs. (43) and (44) are taken over the nearest neighbors of j only. The equation of motion of $\langle\mu_j(t)\rangle$ there contains a higher-order correlation as it always occurs when one deals with a BBGKY hierarchy.[50] The MFA solves Eq. (44) by a factorization approximation to the three-spin correlation

$$\langle\mu_{i_1}(t)\,\mu_{i_2}(t)\,\mu_{i_3}(t)\rangle\approx\langle\mu_{i_1}(t)\rangle\langle\mu_{i_2}(t)\rangle\langle\mu_{i_3}(t)\rangle\quad.\tag{45}$$

Then the equation of motion is conveniently rewritten, again including a magnetic field H_j at lattice site j,

$$\tau_s\frac{d}{dt}\langle\mu_j(t)\rangle=-\langle\mu_j(t)\rangle+\tanh\left[\frac{1}{k_BT}\left(\mu_BH_j'+J\sum_{i(\neq j)}\langle\mu_i(t)\rangle\right)\right]\quad.\tag{46}$$

For temperatures below the critical temperature T_c given by

$$k_BT_c=J(0)=\sum_{i(\neq j)}J_{ij}\,,\quad J(\vec{k})=\sum_{i(\neq j)}J_{ij}\,e^{i\vec{k}\cdot(\vec{r}_i-\vec{r}_j)}\quad,\tag{47}$$

three real stationary solutions $\langle\mu\rangle_1>\langle\mu\rangle_2>\langle\mu\rangle_3$ of Eq. (46) are found as long as H does not exceed the coercive field H^*,

$$\mu_BH^*=-k_BT_c\left(1-\frac{T}{T_c}\right)^{1/2}+k_BT\,\operatorname{arctanh}\left(1-\frac{T}{T_c}\right)^{1/2}\quad.\tag{48}$$

For $H'<0$ the largest solution $\langle\mu\rangle_1$ is "metastable" and $\langle\mu\rangle_3$ is stable, while the intermediate solution $\langle\mu\rangle_2$, where the susceptibility is negative, is unphysical.[66] Using linear-response theory one derives from Eq. (46) the wave-vector- and frequency-dependent susceptibility[4]

$$\chi(\vec{k},\omega)=\frac{\chi_{\vec{k}}}{1+i\omega\tau_{\vec{k}}}\,,\quad\tau_{\vec{k}}=\frac{\tau_s\,k_BT\,\chi_{\vec{k}}}{1-\langle\mu\rangle^2}\quad,\tag{49}$$

where

$$\chi_{\vec{k}}=\frac{1}{k_BT}\,\frac{(1-\langle\mu\rangle^2)}{1-[J(\vec{k})/k_BT](1-\langle\mu\rangle^2)}\quad.\tag{50}$$

It is seen that $\chi_{\vec{k}}$ diverges at $\vec{k}=0$ both for $T\to T_c$ and $H\to H^*$, where the magnetization $\langle\mu\rangle^*$ is given by

$$\langle\mu\rangle^*=(1-T/T_c)^{1/2}\quad.\tag{51}$$

Thus the MFA predicts a "soft mode" associated with the spinodal curve [Eq. (48)]. Being interested mainly in the behavior near the critical point it is legitimate to expand the tanh in Eq. (46) according to $\tanh x\approx x-\frac{1}{3}x^3$. Then Eq. (46) reduces precisely to the time-dependent Ginzburg-Landau equation[4]; in this limit the nonequilibrium relaxation functions and associated lifetimes may be calculated in closed form.[4] As an example we plotted some $\phi(t)$ functions in Fig. 1, and give the relaxation time τ_R' of the metastable state [Eq. (16)] in Fig. 14, again in scaled form, since the DSH [Eq. (28)] is exact in this case.

While the curves of Figs. 1 and 5–8 are qualitatively similar, a quantative comparison exhibits

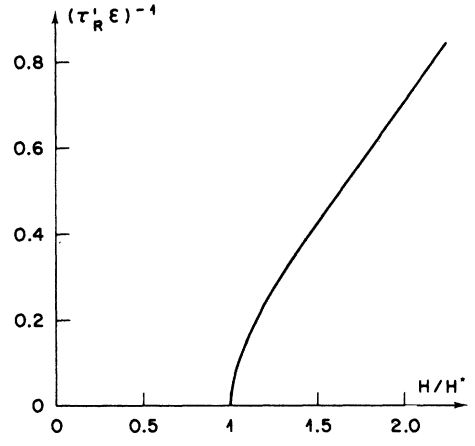

FIG. 14. Scaled inverse relaxation time $(\tau_R^S)^{-1}$ plotted vs the normalized scaled field H^S in the mean-field approximation.

gross differences, as expected. Also the infinite lifetime[3,4,9] of the metastable states is unphysical. While the MFA has a very-well-defined spinodal, no such singularity was detected in the numerical work. If a spinodal also exists in the two-dimensional Ising model as supported by series extrapolations,[6] it can have only a very tiny effect on the magnetization curves (see Fig. 21).

Outside the critical region Eq. (46) may be solved by numerical integration[44]; the behavior is rather similar to that in the critical region, therefore we do not show these results. In order to effect a treatment going beyond the MFA it is possible to keep the three-spin correlation function in Eq. (44), but introduce a factorization in a higher-order equation of motion.[67] An approach of this kind has been worked out numerically,[68] but as expected the results are very similar to the ordinary MFA. We must choose an entirely different approach if we want to be in agreement with the critical properties of the kinetic Ising model.[25,58,59] Sec. IV B is devoted to such an attempt.

B. Theory of cluster dynamics and nucleation

As a first step we reformulate the master equation for the probability distribution of the spins μ_j [Eq. (17)] as a master equation for the probability distribution of clusters a_l^α, where a cluster a_l^α with l spins is characterized by the set of its coordinates on the lattice (denoted symbolically by a_l^α in the spin configuration labelled by α):

$$\frac{dP}{dt}(\{\alpha_1\}, \{\alpha_2\}, \ldots, \{\alpha_l\}, \ldots) = -\sum_j W(\mu_j \to -\mu_j) P(\{a_1^\alpha\}, \{a_2^\alpha\}, \ldots, \{a_l^\alpha\}, \ldots) + \sum_j W(-\mu_j \to \mu_j) P(\{a_1^{\alpha'}\}, \{a_2^{\alpha'}\}, \ldots, \{a_l^{\alpha'}\} \ldots) , \tag{52}$$

where α' is the spin configuration transformed by flip of the jth spin into α. The number of clusters with spins at time t having the configuration α' is denoted by $n_l^\alpha(t)$, and by $\langle \cdots \rangle_\alpha$ we denote the average over all possible spin configurations, weighted with the appropriate Boltzmann factor. Then simple geometric considerations lead to the following system of equations of motion:

$$\begin{aligned}\frac{d}{dt}\langle n_l^\alpha(t)\rangle_\alpha = &\sum_{l_1}\langle n_{l+l_1}^\alpha(t)\, A_{l+l_1,l_1}^\alpha(t)\rangle_\alpha - \sum_{l_1}\langle n_l^\alpha(t)\, B_{l,l_1}^\alpha(t)\rangle_\alpha + \sum_{l_1}\langle n_{l-l_1}^\alpha(t)\, B_{l-l_1,l_1}^\alpha(t)\rangle_\alpha - \sum_{l_1}\langle n_l^\alpha(t)\, A_{l,l_1}^\alpha(t)\rangle_\alpha \\ &+ \sum_{l_1,l_2}\langle n_{l+l_1+l_2}^\alpha(t)\, A_{l+l_1+l_2,l_1,l_2}^\alpha(t)\rangle_\alpha - \sum_{l_1,l_2}\langle n_l^\alpha(t)\, B_{l,l_1,l_2}^\alpha(t)\rangle_\alpha + \sum_{l_1,l_2}\langle n_{l-l_1-l_2}^\alpha(t)\, B_{l-l_1-l_2,l_1,l_2}^\alpha(t)\rangle_\alpha \\ &- \sum_{l_1,l_2}\langle n_l^\alpha(t)\, A_{l,l_1,l_2}^\alpha(t)\rangle_\alpha + \sum_{l_1 l_2 l_3}\langle n_{l+l_1+l_2+l_3}^\alpha(t)\, A_{l+l_1+l_2+l_3,l_1,l_2,l_3}^\alpha(t)\rangle_\alpha - \sum_{l_1 l_2 l_3}\langle n_l^\alpha(t)\, B_{l,l_1,l_2,l_3}^\alpha(t)\rangle_\alpha \\ &+ \sum_{l_1 l_2 l_3}\langle n_{l-l_1-l_2-l_3}^\alpha(t)\, B_{l-l_1-l_2-l_3,l_1,l_2,l_3}^\alpha(t)\rangle - \sum_{l_1 l_2 l_3}\langle n_l^\alpha(t)\, A_{l,l_1,l_2,l_3}^\alpha(t)\rangle_\alpha ,\end{aligned} \tag{53}$$

which is exact for the square lattice, like the BBGKY hierarchy.[50] The first term on the right-hand side of Eq. (53) corresponds to a reaction, where by a single spin flip a cluster with $l+l_1$ spins splits up into two clusters with l and l_1-1 spins. The probability for this reaction is written proportional to the concentration $n_{l+l_1}^\alpha(t)$ of such clusters in that particular configuration and a splitting rate $A_{l+l_1,l_1}^\alpha(t)$ which also depends on the particular configuration. The next term characterizes the inverse reaction, where by a single spin flip a cluster with l spins incorporates a cluster with l_1-1 spins. The corresponding growing rate is $B_{l,l_1}^\alpha(t)$. The third term characterizes the growth of a cluster with size $l-l_1$ to size l, and the fourth term characterizes the inverse reaction. The following reactions involve more than two clusters. On the square lattice a single spin flip can lead at most to a reaction between four clusters. In Eq. (53) the convention is used that l, l_1, l_2, l_3 are positive integers greater than or equal to 1 and $l_1 \geq 2$ in the fifth to twelfth term. Thus Eq. (53) contains all existing reactions.

Aiming at exact solutions Eq. (53) would have no advantage at all in comparison to Eq. (8) [or Eq. (44)]. While the factorization approximation applied to Eq. (44) yielded only the mean-field approximation, a similar factorization approximation applied to Eq. (53) is still consistent with the correct critical behavior. Thus we write

$$\begin{aligned}&\langle n_l^\alpha(t)\rangle_\alpha = n_l'(t) , \\ &\langle n_{l+l_1}^\alpha(t)\, A_{l+l_1,l_1}^\alpha(t)\rangle_\alpha \approx n_{l+l_1}'(t)\,\langle A_{l+l_1,l_1}^\alpha(t)\rangle_\alpha , \\ &\langle n_l^\alpha(t)\, B_{l,l_1}^\alpha(t)\rangle_\alpha \approx n_l'(t)\,\langle B_{l,l_1}^\alpha(t)\rangle_\alpha .\end{aligned} \tag{54}$$

It is seen that by this approximation any influence of the particular configuration α on the reaction rates is lost: This approximation corresponds to a mean-field approximation with respect to the various clusters, while previously we had a mean-field approximation with respect to the bulk homogeneous magnetization itself. For Eqs. (53) and (54) to be tractable, a further assumption about the reaction rates $\langle A_{l+l_1,l_1}^\alpha(t)\rangle_\alpha$, $\langle B_{l,l_1}^\alpha(t)\rangle_\alpha$ must be made. Here $\langle B_{l,l_1}^\alpha(t)\rangle_\alpha$ gives the average rate at which a cluster with l_1-1 spins is incorporated

by a cluster with l spins. We write using the convention $n_0'(t) \equiv 1$:

$$\langle B^{\alpha}_{l,l_1}(t)\rangle_{\alpha} \cong R_l\, n'_{l_1-1}(t)\, b_{l_1-1} \quad , \tag{55}$$

i.e., we assume the l dependence of this reaction is simply given by a time-independent factor $R_l\, b_{l_1-1}$. Furthermore, we assume that $\langle A^{\alpha}_{l+l_1,l_1} \times(t)\rangle_{\alpha}$ is independent of t,

$$\langle A_{l+l_1,l_1}(t)\rangle_{\alpha} = A_{l+l_1} \quad . \tag{56}$$

For these equations still to be consistent with thermal equilibrium as was our original cluster equation (17) because of Eq. (18), we must again require a detailed-balance equation in terms of the equilibrium cluster distributions n_l [see Appendix, Eq. (A1)],

$$n_{l+l_1} A_{l+l_1} = n_l n_{l_1-1} R_l\, b_{l_1-1} \quad . \tag{57}$$

Similar relations can be written down for all the other reactions involved in Eq. (53), but in view of the crudeness of the approximations Eqs. (54)–(56) it seems legitimate to neglect all reactions in which more than two clusters are involved. Writing

$$c_l(t) = n_l'(t)/n_l \tag{58}$$

one has

$$\begin{aligned} n_l \frac{dc_l(t)}{dt} = {} & R_l n_l \Big[\sum_{l_1} b_{l_1-1}\, n_{l_1-1}\, c_{l+l_1}(t) \\ & - c_l(t) \sum_{l_1} b_{l_1-1}\, n_{l_1-1}\, c_{l_1-1}(t)\Big] \\ & + \sum_{l_1} c_{l-l_1}(t)\, b_{l_1-1}\, R_{l-l_1}\, n_{l_1-1}\, c_{l_1-1}(t)\, n_{l-l_1} \\ & - c_l(t) \sum_{l_1} n_{l-l_1}\, R_{l-l_1}\, b_{l_1-1}\, n_{l_1-1} \, , \\ & l = 1, 2, 3, \ldots . \end{aligned} \tag{59}$$

Thus we have derived a coupled nonlinear system of first-order differential equations which can be solve numerically if a guess about the coefficients b_{l_1-1} and effective reaction rates R_l is made. Instead of trying this we rather point out the relation to the more conventional nucleation theories.[35–41] The most simple approximation to Eq. (59) is found if the cluster concentrations are very small: Then the dominant term in the sums in Eq. (59) is clearly the $l_1 = 1$ contribution, since $n_0 \equiv 1$ while $n_l \ll 1$ for $l \neq 0$, so that one can write

$$\begin{aligned} n_l \frac{dc_l(t)}{dt} = {} & R_l n_l b_0 \left[c_{l+1}(t) - c_l(t)\right] \\ & + R_{l-1}\, n_{l-1}\, b_0 \left[c_{l-1}(t) - c_l(t)\right] \quad , \end{aligned} \tag{60}$$

which is precisely the well-known Becker-Döring nucleation equation of the classical nucleation theory.[35,41] From the condition $n_l \ll 1$ we see that it can be correct only far from the critical point.

In order to account also for the critical behavior a better approximation is needed. Bearing in mind the study of the growth of a cluster to critical or supercritical size in the metastable phase, it is reasonable to assume that the smaller clusters with which this cluster reacts have the concentration $c_{l_1-1}(t) = 1$ corresponding to "metastable equilibrium" [see Appendix, especially Fig. 23]. Then Eq. (59) reduces to a system of equations first given by Katz *et al.*[69]

$$\begin{aligned} \frac{1}{R_l}\frac{dc_l(t)}{dt} = {} & \sum_{l_1} b_{l_1-1}\, n_{l_1-1} \left[c_{l+l_1}(t) - c_l(t)\right] \\ & + \sum_{l_1} \frac{n_{l-l_1}}{n_l} \frac{R_{l-l_1}}{R_l}\, b_{l_1-1}\, n_{l-1} \\ & \times \left[c_{l-l_1}(t) - c_l(t)\right], \quad l = 1, 2, 3, \ldots . \end{aligned} \tag{61a}$$

If one assumes that the distribution $b_{l_1} n_{l_1}$ is rather sharply peaked at some value $l = \tilde{l}$, one may replace Eq. (61a) by the simpler equation[28,70]

$$\begin{aligned} \frac{1}{R_l}\frac{dc_l(t)}{dt} = {} & \tilde{b}\left[c_{l+\tilde{l}}(t) - c_l(t)\right] + \tilde{b} \\ & \times \frac{R_{l-\tilde{l}}}{R_l} \frac{n_{l-\tilde{l}}}{n_l} \left[c_{l-\tilde{l}}(t) - c_l(t)\right] \quad . \end{aligned} \tag{61b}$$

It is hard to say if this approximation is appropriate to the kinetic Ising case, however. Although this system of equations [Eqs. (61)] is already linear in the cluster concentrations, explicit solutions are known only numerically. As a last step of simplification we thus replace the system of difference equations by a differential equation, introducing the expansions[28,41]

$$\begin{aligned} c_{l+l_1}(t) &= c_l(t) + l_1 \frac{\partial c_l(t)}{\partial l} + \tfrac{1}{2} l_1^2 \frac{\partial^2 c_l(t)}{\partial l^2} \quad , \\ n_{l-l_1} R_{l-l_1} &= n_l R_l - l_1 \frac{\partial}{\partial l}\left(n_l R_l\right) \quad , \end{aligned} \tag{62}$$

so that Eq. (61) reduces to

$$\left(\sum_{l_1} l_1^2 b_{l_1-1} n_{l_1-1}\right)^{-1} \frac{\partial n_l(t)}{\partial t} = \frac{\partial}{\partial l}\left(n_l R_l \frac{\partial}{\partial l}\frac{n_l'(t)}{n_l}\right) \quad , \tag{63}$$

where only some effective average $\tilde{b}\,\tilde{l}^2$ enters

$$\tilde{b}\,\tilde{l}^2 \equiv \sum_{l_1} l_1^2\, b_{l_1-1}\, n_{l_1-1} \quad . \tag{64}$$

Equation (64) means essentially that on the average clusters of size $\tilde{l}$ are involved in cluster-cluster reactions. Equation (63) is essentially the nucleation equation postulated by Katz *et al.*[69] and by Kiang *et al.*,[28] but in the kinetic Ising model it is not clear how to determine the temperature dependence of the scale factor $\tilde{b}\,\tilde{l}^2$. Putting $\tilde{b}\,\tilde{l}^2$ equal to b_0 reduces Eq. (63) again to a standard equation of the classical nucleation theory.[41] Thus we follow essentially the standard arguments of this theory to estimate the rate at which large clusters are built

up from the metastable phase.

We note that Eq. (63) is a generalized one-dimensional diffusion equation in the "space" of cluster sizes $\{l\}$, which is written as continuity equation

$$\frac{\partial n_l'(t)}{\partial t}+\frac{\partial J_l}{\partial l}=0 \tag{65}$$

for a current, J_l,

$$J_l = D_l \frac{\partial n_l(t)}{\partial l}+v_l n_l'(t) \quad , \tag{66}$$

where a "diffusion constant" D_l and "drift velocity" v_l are introduced,

$$D_l = \tilde{b}\,\tilde{l}^2 R_l\,, \quad v_l = -D_l \frac{\partial \ln(n_l)}{\partial l} \quad . \tag{67}$$

It is important to note that v_l changes its sign at l^*.

Using Eqs. (65)–(67) we can make the qualitative picture about nucleation drawn in Sec. III B more precise: cluster growth is described as a diffusion over a potential barrier of height f_l^*. The drift term always goes "downhill" and thus leads to disintegration of subcritical ($l<l^*$) clusters, while supercritical clusters ($l>l^*$) are stable against dissociation and tend to grow.

It is seen that Eq. (65) has a steady-state solution with nonzero current $J_l \equiv \tilde{J}$ which is called the nucleation rate.[41] It is found integrating the current with respect to l,

$$-\frac{1}{\tilde{b}\,\tilde{l}^2}\tilde{J}\int_{\tilde{l}}^{\infty}\frac{1}{R_l n_l}\,dl=\int_{\tilde{l}}^{\infty}\frac{\partial c_l}{\partial l}\,dl=c_\infty - c_{\tilde{l}} \quad , \tag{68}$$

which leads to

$$\tilde{J}=\tilde{b}\,\tilde{l}^2\Big/\int_0^{\infty}\frac{dl}{R_l n_l} \tag{69}$$

because of $c_{\tilde{l}}=1$, $c_\infty=0$ (very large clusters form the new phase and are thus removed from the metastable phase per definition). Expanding

$$R_l n_l = R_{l*}\,n_{l*}\left(1+\frac{1}{2n_l^*}\left.\frac{\partial^2 n_l}{\partial l^2}\right|_{l^*}(l-l^*)^2+\cdots\right) \tag{70}$$

it is found that

$$\tilde{J}=\tilde{b}\,\tilde{l}^2\frac{\pi}{\sqrt{2}}R_{l*}\,n_{l*}\left(\frac{1}{n_l}\left.\frac{\partial^2 n_l}{\partial l^2}\right|_{l*}\right)^{1/2}, \tag{71}$$

and assuming a power law introducing a new exponent γ

$$R_l \approx \hat{R}\,l^{\sigma} \tag{72}$$

one may rewrite Eq. (71) with the help of Fisher's droplet model [Eqs. (A1) and (A2)] to find

$$\tilde{J}=\frac{\pi}{\sqrt{2}}\,\tilde{b}\,\tilde{l}^2\,\hat{R}\,q_0(\sigma-1)\left(\frac{a\sigma J}{k_B T}\right)^{(i)}$$
$$\times\epsilon^{3\gamma+4\beta-\gamma\sigma(\gamma+\beta)}\left(\frac{-2\mu_B H_s}{k_B T}\right)^{(j)}$$
$$\times\exp\left[-(\gamma+\beta-1)\left(a\sigma\frac{J}{k_B T}\right)^{(\gamma+\beta)/(\gamma+\beta-1)}\right.$$
$$\left.\times\left(\frac{-2\mu_B H_s}{k_B T}\right)^{-1/(\gamma+\beta-1)}\right] \quad , \tag{73}$$

where

$$(i)=\frac{\gamma\sigma(\gamma+\beta)}{\gamma+\beta-1}-\frac{\frac{5}{2}\gamma+\frac{7}{2}\beta}{\gamma+\beta-1} \quad ,$$

$$(j)=\frac{3\gamma+4\beta-\frac{1}{2}}{\gamma+\beta-1}-\frac{\gamma\sigma(\gamma+\beta)}{\gamma+\beta-1} \quad .$$

It is seen that the nucleation rate obeys the scaling hypothesis[28,71]

$$\tilde{J}(\epsilon, H)=\epsilon^j J_S(H_S) \quad , \tag{74}$$

but its scaling power j can hardly be determined from the crude arguments sketched above. While one may argue that most of the cluster-cluster reactions in which we are interested occur at the cluster surfaces and thus the unknown exponent γ should be close to 1, we know no simple argument to determine the ϵ dependence of $\tilde{b}\,\tilde{l}^2$. We thus treat j as an adjustable parameter.

Now we are dealing with the lifetime of a metastable state. Common belief is that a metastable state corresponds in a sense to the steady-state solution of Eq. (65). The larger the nucleation rate $\tilde{J}$ the smaller will be the lifetimes of this metastable state. In order to make this opinion more quantitative, we recall a simple argument of phase separation kinetics.[36,40,43] One considers the system as being composed of two phases, the metastable phase (with positive magnetization) and the stable phase (with negative magnetization), the latter consisting of all the supercritical clusters, in which the local equilibrium corresponding to the stable phase is established at an early stage of the process already. The magnetization of the total system is decreased by the growth of these supercritical clusters, whose number also increases due to critical clusters originating from the metastable fraction of the system at a rate, $\tilde{J}$. For the fraction $X(t)$ of the stable phase it is written

$$dX=(1-X)\,V(t,t')\,\tilde{J}\,dt' \quad , \tag{75}$$

where $V(t,t')$ is the volume of a domain of the new phase at time t originating from a critical cluster which was built up at time t'. The growth of supercritical clusters is described by the velocity v_l (for $l \gg l^*$ the diffusion may be neglected), and thus one writes for the increase in volume dV of such a cluster

$$dV=v_l dt \equiv \tilde{b}\,\tilde{l}^2 R_l\frac{-2\mu_B H}{k_B T}dt \quad . \tag{76}$$

Considering the regime where $l^* \gg \xi^d$ (d being the dimensionality of the system) one assumes

$$V_l \sim l, \quad R_l \sim l^{1-1/d} \tag{77}$$

and finds from Eqs. (76) and (77)

$$V(t,t) = (g\tilde{b})^d \epsilon^{d(\gamma+\beta)} (\tilde{l})^{2d} (-2H_S/k_BT)^d (t-t')^d \quad . \tag{78}$$

Now Eq. (75) is readily integrated to yield

$$X(t) = 1 - \exp\left[\frac{1}{d+1}[g\tilde{b}\tilde{l}^2\epsilon^{\gamma+\beta}]^d \left(\frac{-2\mu_B H_S}{k_BT}\right)^d \tilde{J}\, t^{d+1}\right]$$

$$= 1 - \exp\left[-\left(\frac{t}{\tau_R}\right)^{d+1}\right] \quad , \tag{79}$$

and one finds for the inverse relaxation time τ_R^{-1} ($-2\mu_B H_S/k_BT < 1$):

$$\tau_R^{-1} = \tilde{b}\tilde{l}^2\epsilon^{(k)}\left[\frac{\pi\hat{R}g^d(\sigma-1)^{1/2}}{(d+1)\sqrt{2}} q_0 \left(a\sigma\frac{J}{k_BT}\right)^{(l)}\right]^{1/(d+1)} \left(\frac{-2\mu_B H_S}{k_BT}\right)^{(m)} \exp\left[-\frac{\gamma+\beta-1}{d+1}\left(a\sigma\frac{J}{k_BT}\right)^{(\gamma+\beta)/(\gamma+\beta-1)} \times \left(\frac{-2\mu_B H_S}{k_BT}\right)^{-1/(\gamma+\beta-1)}\right] \quad , \tag{80}$$

where

$$(k) = \gamma+\beta+\frac{2\gamma+3\beta-\gamma\sigma(\gamma+\beta)}{d+1} \quad ,$$

$$(l) = \frac{\gamma\sigma(\gamma+\beta)}{\gamma+\beta-1} - \frac{5\gamma/2+7\beta/2}{\gamma+\beta-1} \quad ,$$

$$(m) = \frac{d}{d+1} + \frac{1}{d+1}\left(\frac{3\gamma+4}{\gamma+\beta-1} - \frac{\gamma\sigma(\gamma+\beta)}{\gamma+\beta-1}\right) .$$

It is seen that $\tilde{b}\tilde{l}^2$ should diverge with an exponent close to $(\gamma+\beta)/d$, in order that the DSH assumption [Eq. (28)] be fulfilled. If one works with nongeometric clusters [Eqs. (A16), (A18), and (A20) instead of Eq. (77)] one obtains slightly different exponents for the time dependence and magnetic field dependence in Eqs. (79) and (80). If we were able to calculate the correct dependence of $\tilde{b}\tilde{l}^2$ we could attempt to estimate the exponent of the "kinetic slowing down"[22]; in view of the numerous approximations involved in the whole treatment this task seems premature, however, and we just postulate the appropriate ϵ dependence for $\tilde{b}\tilde{l}^2$ to write

$$(\tau_R^S)^{-1} = (\text{const})\left(\frac{-2\mu_B H_S}{k_BT}\right)^{(n)} \times \exp\left[-\frac{\gamma+\beta-1}{d+1}\left(a\sigma\frac{J}{k_BT}\right)^{(\gamma+\beta)/(\gamma+\beta-1)} \times \left(\frac{-2\mu_B H_S}{k_BT}\right)^{-1/(\gamma+\beta-1)}\right] \quad [(-2\mu_B H_S/k_BT) < 1] \, , \tag{81a}$$

where

$$(n) = \frac{d}{d+1} + \frac{d}{d+1}\,\frac{2\gamma+3\beta-\frac{1}{2}+(\gamma+\beta)/d}{\gamma+\beta-1} \, .$$

The restriction $-2\mu_B H_S/k_BT < 1$ in Eqs. (73), (80), and (81) is due to the approximate calculation of l^* [Eq. (A21)]. Since our data belong to the region $-\mu_B H_S/k_BT > 1$, however, we calculate the correct l^* numerically from $(\partial n_l/\partial l)|_{l^*} \equiv 0$ using Eq. (A1) and take this l^* in Eq. (71) to derive a result analogous to Eq. (81a) which is also valid for $-2\mu_B H_S/k_BT > 1$,

$$(\tau_R^S)^{-1} = (\text{const})\left(\frac{-2\mu_B H_S}{k_BT}\right)^{d/(d+1)} (l^*\epsilon^{\gamma+\beta})^{(\sigma/2-1/d-\tau)/(d+1)} \times \exp\left(\frac{2(1-\sigma)l^*\mu_B H}{(d+1)\sigma k_BT}\right) , \tag{81b}$$

which reduces to Eq. (81a) using the approximation [Eq. (A21)]. Equation (81b) is plotted in Fig. 11. Since very crude approximations were necessary to derive this formula, the excellent agreement with the data might be somewhat fortuitous. But note that the treatment of this section is still consistent with nonclassical critical exponents, in contrast to the mean-field approximations.

Equations (81) predicts a completely smooth behavior of the lifetime, as the same as Eq. (A22) predicts a smooth behavior of the magnetization. An unambiguous definition of a coercive field H_S^* (or limit of metastability) is impossible in the framework of this theory. The possibility that a coercive field H_S^* exists where $\partial\langle\mu\rangle/\partial H$ and τ_R^S have singularities (e.g., a divergent slope) cannot be ruled out by the present treatment, since these singularities might well have been lost in the long succession of approximations leading from Eq. (53) to Eqs. (81). It is certainly very hard to justify properly the various assumptions made, and it was not the purpose to present a correct quantitative theory of nonequilibrium dynamics of the kinetic Ising model in this section, but rather elucidate the extremely crude approximations inherent in the various phenomenological formulations of nucleation theory.[28,29,35–41,70,71]

C. Comparison of theory of cluster dynamics with computer experiment

By the treatment leading from Eqs. (61) to Eqs. (81) we have been able to estimate the relaxation time of the system. It is also interesting to investigate the dynamics of the cluster distribution $n_l'(t) = n_l c_l(t)$ in more detail. Here Eqs. (61) have to be

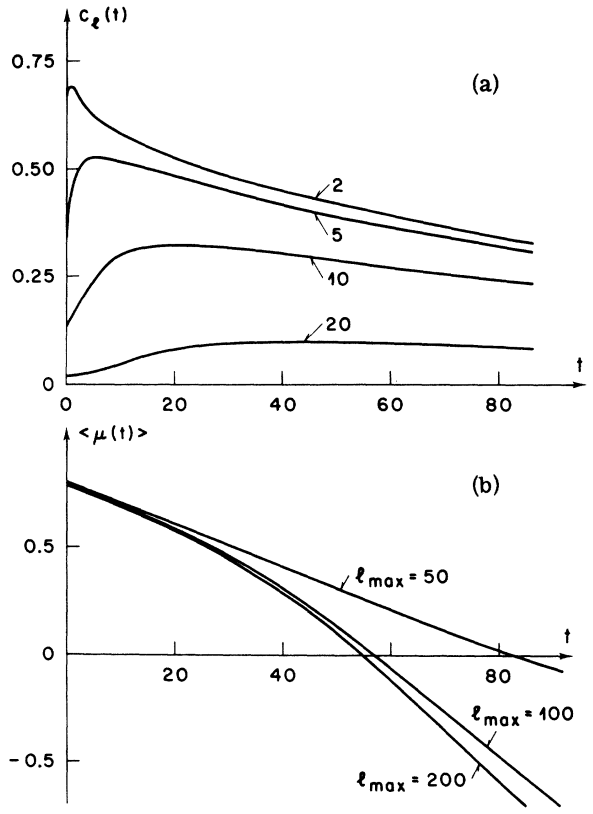

FIG. 15. (a) Normalized cluster concentrations $c_l(t)$ according to linearized nucleation theory [Eq. (60)] plotted vs time (in arbitrary units), for $\epsilon = 0.026$ and $\mu_B H/k_B T = -0.10$. Parameter of the curves is l. Curves for $l_{max} = 100$, 200, and 400 agree with each other. (b) Magnetization $\langle\mu(t)\rangle$ plotted vs time, as calculated from the $c_l(t)$ shown in Fig. 15(a). Curves for various values of l_{max} are shown.

solved numerically, but note that its solution provides only the concentration of clusters inside the fraction of the system, which is still in the metastable phase. The concentration of clusters related to the total system is then

$$n_l^{\text{nonl}}(t) = n_l'(t)\,[1 - X(t)] \quad , \tag{82}$$

which is a crude way [like Eq. (75)] of taking the nonlinearity of the problem into account, and avoided replacing Eq. (59) by Eq. (61). In order to have consistency we should not use Eq. (79) in the present context but require that $X(t)$ be determined self-consistently by

$$X(t) = \sum_{l=1}^{\infty} l\,[n_l^{\text{nonl}}(t) - n_l(H')] \times\left(1 - \sum_{l=1}^{\infty} l n_l(H') - \sum_{l=1}^{\infty} l n_l(H)\right)^{-1} . \tag{83}$$

No attempt has been made to solve Eqs. (61), (82), and (83) numerically, however, because of the lack of safe knowledge about the coefficients b_l. In fact, even the simple Eq. (60) has been studied in extremely simple cases only[72,73]; using the Frenkel droplet model[38] and requiring the boundary conditions[72]

$$c_{l_{\min}}(t) = 1 \quad , \tag{84}$$

$$n_{l_{\max}} \frac{dc_{l_{\max}}(t)}{dt} = R_{l_{\max}-1}\, n_{l_{\max}-1}\, b_0 \times [c_{l_{\max}-1}(t) - c_{l_{\max}}(t)] \quad , \tag{85}$$

with one choice of $l_{\min}$ and $l_{\max}$ only ($l_{\min} = 10$, $l_{\max} = 110$). The purpose of this treatment was to study in which way $\tilde{J}$ and $n_l'(t)$ reach their saturation value in an open system where nucleation processes

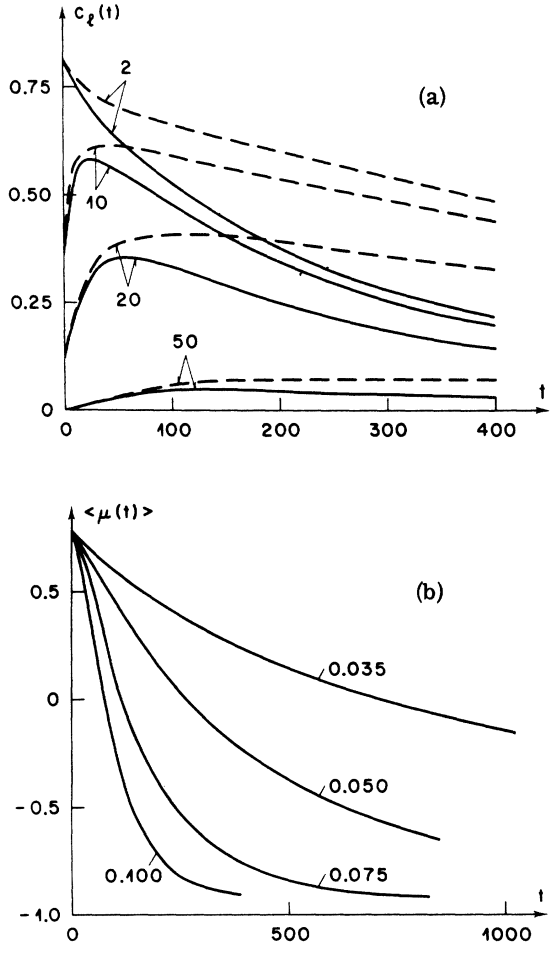

FIG. 16. (a) Normalized cluster concentrations $c_l(t)$ according to linearized nucleation theory [Eq. (60), broken curves] and according to the nonlinear theory [Eq. (82), full curves]. All parameters have the same value as in Fig. 15(a). (b) Magnetization $\langle\mu(t)$ plotted vs time, as calculated from the nonlinear approximation [Eqs. (82) and (83)] for $l_{max} = 100$ and $\epsilon = 0.026$. Parameter of the curves is $-\mu_B H/k_B T$.

occur. The boundary condition $c_{l_{\min}}(t)=1$ is hardly appropriate in the Ising case, and we thus replace Eq. (84) by

$$n_{l_{\min}}\frac{dc_{l_{\min}}(t)}{dt}=R_{l_{\min}}b_0\,[c_{l_{\min}+1}(t)-c_{l_{\min}}(t)]n_{l_{\min}} \tag{86}$$

and choose $l_{\min}=1$. While Eq. (60) with the boundary conditions [Eqs. (84) and (85)] leads to a steady-state solution

$$c_l(t)=1 \quad t\to\infty \quad l=l_{\min},\ldots,l_{\max}\ , \tag{87}$$

we get another steady-state solution for Eq. (60) with the boundary condition Eqs. (85) and (86)

$$c_l(t)=\text{const}<1,\ t\to\infty,\ l=l_{\min},\ldots,l_{\max}; \tag{88}$$

thus we investigated the problem posed by Eqs. (60), (85), and (86), where we took for n_l the Fisher droplet model Eq. (A1) and considered various $l_{\max}$ ($l_{\max}=50$, 100, 200, and 400). As an example we show $c_l(t)$ for $r=1$ [Eq. (72)] and $-H/k_BT=0.1$, $\epsilon=0.026$, in Fig. 15(a). The unknown constants b_0 and $\hat{R}$ are incorporated in the arbitrary time scale. Time integrations were performed using CSMPIII[74] routines. No dependence on $l_{\max}$ was found for the small clusters found in the figure. While $c_1(t)$ is monotonically decreasing, other $c_l(t)$ reach a maximum and then decrease again. For larger l this maximum is extremely flat. If we calculate the magnetization

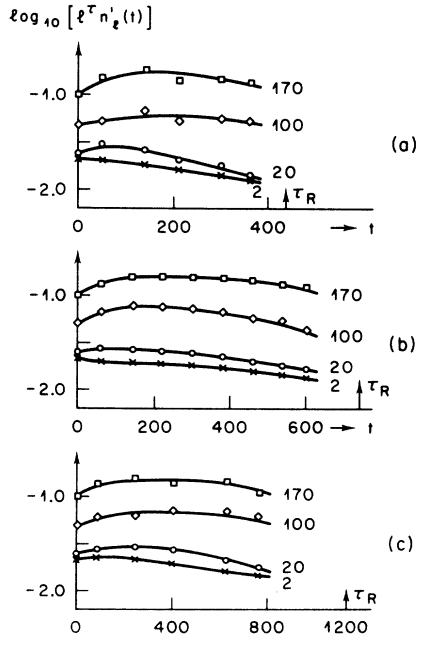

FIG. 17. Simulated cluster concentrations $l^\tau n_l'(t)$ plotted vs time for $J/k_BT=0.45$ and the fields $\mu_BH/k_BT=-0.015$ (*a*), -0.010 (*b*), and -0.0075 (*c*). Parameter of the curves is l. The arrow indicates the magnitude of the corresponding relaxation time τ_R.

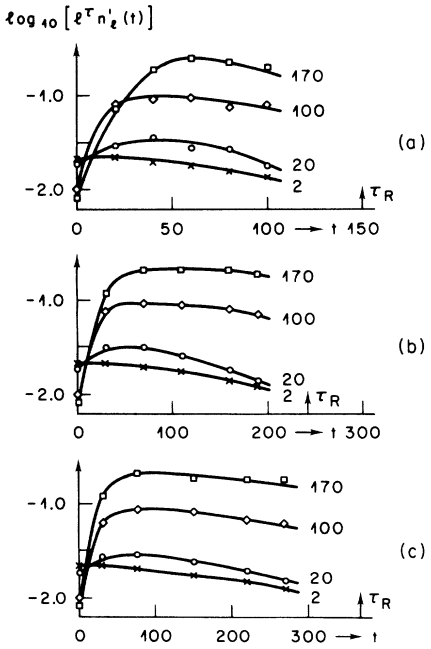

FIG. 18. Simulated cluster concentrations $l^\tau n_l'(t)$ plotted vs time for $J/k_BT=0.46$ and the fields $\mu_BH/k_BT=-0.040$ (*a*), -0.030 (*b*), and -0.022 (*c*). Parameter of the curves is l. The arrow indicates the magnitude of the corresponding relaxation time τ_R.

from this linear cluster dynamics according to Eq. (27), as done in Fig. 15(b), we find a pronounced dependence on $l_{\max}$ for longer times, where the contributions of larger clusters have a notable effect. Here $\langle\mu(t)\rangle$ does not reach the equilibrium at the correct negative value, however, but rather decreases to a large negative value for $t\to\infty$, since Eq. (61) is strictly linear. Thus this description makes sense for the initial stages of the process only.

Similar results are obtained for other values of r and $-2\mu_BH/k_BT$ investigated. For smaller values of $-2H\mu_B/k_BT$ where $l^*\lesssim l_{\max}$, also the cluster distribution $n_l'(t)$ depends on $l_{\max}$. If $l_{\max}\ll l^*$, one finds that the steady-state solution of Eq. (60) leads to a final state with positive magnetization. This type of metastability is clearly a finite size effect and of no particular interest to us here.

In Fig. 16 we now consider the improvement obtained by the excluded volume-nonlinearity effect obtained by the use of Eqs. (82) and (83) together with Eqs. (60), (85), and (86). Here $c_l^{\text{nonl}}(t)\equiv n_l^{\text{nonl}}(t)/n_l$ is plotted versus time for various l at $\epsilon=0.026$, $-\mu_BH/k_BT=0.05$. Evidently the results of the nonlinear approximation (full curves) are distinctly different from the linear approximation (dashed curves). Here the cluster concentrations do not reach a saturation value but decrease to zero for $t\to\infty$.

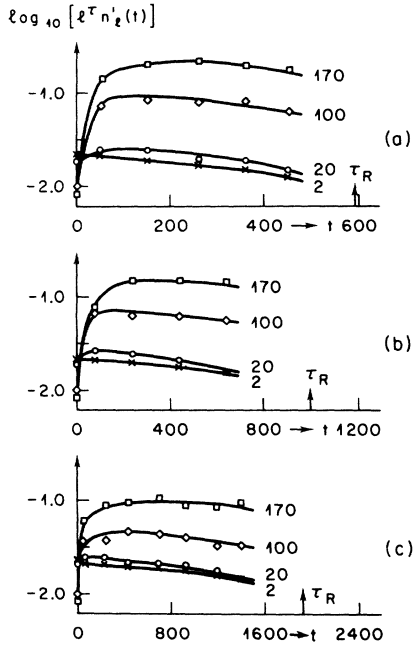

FIG. 19. Simulated cluster concentrations $l^{\tau}n_l'(t)$ plotted vs time for $J/k_BT = 0.46$ and the fields $\mu_BH/k_BT = -0.015(a)$, $-0.012(b)$, and $-0.008(c)$. Parameter of the curves is l. The arrow indicates the magnitude of the correspondin relaxation time τ_R.

In Fig. 16 we plot several of the nonequilibrium relaxation functions $\phi(t) \equiv X(t)$ from this treatment. Although the qualitative behavior of these functions is similar to the results of the computer simulation for larger values of $-\mu_BH/k_BT$, quantitative comparison is premature, since $\phi(t)$ derived from Eqs. (60), (82), (83), (85), and (86) still distinctly depends on the values of l_{max} used. There is clearly a need for better boundary conditions than Eqs. (84)–(86). We do not follow this question here further, however, but rather discuss now the results of the computer simulation for the time-dependent cluster distribution $n_l'(t)$. One example has already been given in Fig. 13, and further results are displayed in Figs. 17–20. Here $\log_{10}[l^{\tau}n_l'(t)]$ is plotted versus time for various l, μ_BH/k_BT, and J/k_BT. Deriving these results, averages are taken over finite intervals $\Delta l(l)$ and Δt in order to have reasonable statistics. Nevertheless some scatter in the data points is still present (mainly at $J/k_BT = 0.45$, the temperature closest to T_c. The position of τ_R (where also $\langle \mu(t) \rangle \approx 0$) is marked by an arrow. It is seen that the smallest clusters decrease steadily, while clusters with intermediate size exhibit a flat maximum and then decrease again. Comparing these curves to the results of the simplest nucleation theory [Figs. (15 and 16)] we note that the maxima in the actual $n_l'(t)$ curves are considerably flatter than predicted. The steep increase of the $n_l'(t)$ for small t does not occur in the computer experiment very near T_c. This discrepancy is due to the neglect of all higher-order reactions between clusters in Eq. (60); here clusters can grow and shrink in steps of one spin only and already the direct observation of the development of the spin configurations demonstrates that this assumption of the conventional nucleation theories does not hold for the kinetic Ising model.[21]

D. Scaling proposal for analytic continuation

Having established the existence of well-defined metastable states in the kinetic Ising model which are independent of the size of the model system and having established that the nonequilibrium relaxation functions satisfy the dynamic scaling hypothesis, it is natural to attempt a construction of, at least, some properties of the metastable states by an extrapolation of the scaling equation of state.[75] Note that the two approximate approaches, sketched so far, yielded results quite inconsistent with each other; the mean-field approximation yielded a spinodal curve with divergent susceptibility separating metastable from instable states, while the nucleation treatment predicted a completely smooth "disappearance" of metastability

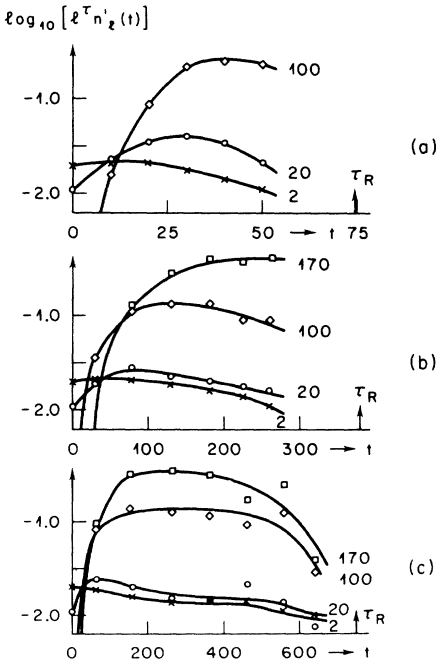

FIG. 20. Simulated cluster concentrations $l^{\tau}n_l'(t)$ plotted vs time for $J/k_BT = 0.48$ and the fields $\mu_BH/k_BT = -0.100$ (a), -0.040 (b), and -0.022 (c). Parameter of the curves is l. The arrow indicates the magnitude of the corresponding relaxation time τ_R.

with increasing values of $-\mu_B H/k_B T$. The latter theory did not give any indication of a well-defined coercive field. But series extrapolations[6] are consistent with the existence of a spinodal also in the Ising model, and experimental data can also be extrapolated to yield "pseudospinodal" curves.[7] Thus it is worthwhile studying these possibilities of extrapolation from the equilibrium properties in greater generality; this may be achieved most conveniently using the Schofield representation of variables[76]:

$$H = a' r^{\beta\delta}\theta(1-\theta^2), \quad -\epsilon = r(1-b^2\theta^2) \quad , \tag{89}$$

where b is an arbitrary constant and a' is related to the critical amplitudes of magnetization (B) and susceptibility above T_c (C_0) by

$$a' = B(b^2-1)^{\beta}/C_0 \quad . \tag{90}$$

In this parametric transformation the singularities for $T \to T_c$, $H \to 0$ are replaced by the singular behavior as $r \to 0$ (which is something like a radius measuring the distance from the singular point), while the "angular" dependence on θ has no singular behavior (except perhaps at the coexistence curve, $\theta = 1$; this occurs, for example, in the spherical and Heisenberg model where the zero-field susceptibility below T_c diverges). The homogeneity requirement for the equation of state is now given by[27,76]

$$\langle\mu\rangle/r^{\beta} = \theta f(\theta^2) \quad , \tag{91}$$

where $f(\theta)$ is essentially the scaling function. Note that θ transforms into the scaled field H_s by

$$-H_s/a' = \theta(\theta^2-1)/(b^2\theta^2-1)^{\beta\delta} \quad . \tag{92}$$

The metastable states we are seeking are states with a positive magnetization in a negative field and thus correspond to values of $\theta > 1$. If at $\theta = 1$, $f(\theta^2)$ has an essential singularity as conjectured from the droplet model, the analytic continuation of $f(\theta^2)$ for $\theta > 1$ should be complex. Such a complex continuation was indeed possible in a special case[8] where the imaginary part could be related to the lifetime. Since the droplet model also predicts that all derivatives of $\langle\mu\rangle$ with respect to H at $H \to 0+$ exist, it is fair to expect that the imaginary part is extremely small for small negative H, and becomes appreciable only at the coercive field H^* where states start to be unstable. What we try is thus a real extrapolation of $f(\theta^2)$ with a value θ^* corresponding to H_s^*. This implies that the coercive field H^* varies as $\epsilon^{\beta\delta}$, and the order parameter $\langle\mu\rangle^*$ at H^* varies as ϵ^{β}, with the same exponent as the order parameter at the coexistence curve; only the critical amplitude should be different. Now we note that for fixed b there exists a maximum value of $-H_s$ which can be reached by the transformation Eq. (92) with real θ. It is convenient if this maximum value coincides with $-H^*$, which is achieved choosing

$$b^2 = \frac{1}{\theta^{*2}} \frac{3\theta^{*2}-1}{(2\beta\delta-1)+\theta^{*2}(3-2\beta\delta)} \quad . \tag{93}$$

Note that the mean-field case ($\beta = \frac{1}{2}$, $\delta = 3$), where the equation of state is known explicitly,

$$C_0 H = (-\epsilon)\langle\mu\rangle + B^{-2}\langle\mu\rangle^3 \quad , \tag{94}$$

is exceptional since here we may take $b^2 = \frac{3}{2}$ to have $\theta^* = \infty$. In this case $f(\theta^2) = \text{const}$, i.e., the scaling function $\theta f(\theta^2)$ is precisely linear.[77] In order to discuss the singularity at θ^* in the general case we study the susceptibility

$$\begin{aligned}\chi &= \left.\frac{\partial\langle\mu\rangle}{\partial H}\right|_T \\ &= \beta r^{\beta-1}\theta f(\theta^2)\Big/\left.\frac{\partial H}{\partial r}\right|_{\epsilon} \\ &\quad + r^{\beta}[f(\theta^2)+2\theta^2 f'(\theta^2)]\Big/\left.\frac{\partial H}{\partial\theta}\right|_{\epsilon} \quad ,\end{aligned} \tag{95}$$

which is found to be[76]

$$\chi = \frac{r^{-\gamma}}{a'} \frac{(1-b^2\theta^2)2\theta^2 f'(\theta^2) + [1-b^2\theta^2(1-2\beta)]f(\theta^2)}{1+\theta^2(2b^2\beta\delta-b^2-3)+b^2\theta^4(3-2\beta\delta)} \quad . \tag{96}$$

Using Eq. (94) this is further rewritten

$$\chi = \frac{r^{-\gamma}}{a'} \frac{(1-b^2\theta^2)2\theta^2 f'(\theta^2) + [1-(1-2\beta)b^2\theta^2]f(\theta^2)}{(1-\theta^2/\theta^{*2})[1+\theta^2\theta^{*2}b^2(2\beta\delta-3)]} \quad . \tag{97}$$

In this form the behavior at the coercive field H^* is conveniently discussed, assuming that

$$f(\theta^2) \approx f_0(1-\theta^2/\theta^{*2})^{(1+2\Psi)} + \text{const}, \quad \theta \to \theta^* \quad , \tag{98}$$

where $\Psi \geq -\frac{1}{2}$ since the magnetization must be finite. If $(1-2\beta)b^2\theta^{*2} \neq 1$ it is found that χ diverges from $-\frac{1}{2} \leq \Psi < \frac{1}{2}$,

$$\chi \propto (H-H^*)^{-1/2+\Psi}, \quad H \to H^{*+} \quad , \tag{99}$$

while χ has a cusp for $\frac{1}{2} \leq \Psi < \frac{3}{2}$,

$$\left.\frac{\partial\chi}{\partial H}\right|_{\epsilon} \propto -(H-H^*)^{-3/2+\Psi} \quad H \to H^{*+} \quad . \tag{100}$$

A cusp is also found in the regular case $\Psi = -\frac{1}{2}$ if $(1-2\beta)b^2\theta^{*2} = 1$; this is precisely the situation of the linear model equation of state,[77] where it is assumed (for nonclassical exponents)

$$b^2 = \frac{(\delta-3)}{(\delta-1)(1-2\beta)}, \quad f(\theta^2) \equiv f_0 \quad , \tag{101}$$

so that[77]

$$\chi = C_0 r^{-\gamma} \frac{1}{1+\theta^2(2\beta\delta-3)/(1-2\beta)} \quad . \tag{102}$$

From Eqs. (93) and (101) we get

$$\theta^{*2}=\frac{\delta-1}{\delta-3},\quad H^*=-a'\epsilon^{\beta\delta}\left(\frac{\delta-1}{\delta-3}\right)^{1/2}\left(\frac{1-2\beta}{2\beta}\right)^{\beta\delta}\times\frac{2}{\delta-3}\ , \tag{103}$$

and

$$\langle\mu\rangle^*=a'C_0\left(\frac{\delta-1}{\delta-3}\right)^{1/2}\left(\frac{1-2\beta}{2\beta}\right)^{\beta}\epsilon^{\beta}\ . \tag{104}$$

For $d=2$, $\langle\mu\rangle^*\cong 1.18\,\epsilon^{0.125}$. Equation (102) leads to

$$\chi^*=C_0\epsilon^{\gamma}\left(\frac{2}{1-2\beta}\right)^{\gamma}\frac{\delta+6\beta-2\beta\delta-3}{\beta\delta^2-2\beta\delta+3\beta-\delta}\ , \tag{105}$$

and

$$\left.\frac{\partial\chi}{\partial H}\right|_{\epsilon}\xrightarrow{H\to H^*}-\epsilon^{(\beta-3\gamma)/2}(H-H^*)^{-1/2}-\frac{1}{2}\frac{C_0}{(2a')^{1/2}}\times\left(\frac{1-2\beta}{2\beta}\right)^{(3\gamma-\beta)/2}\left(\frac{\delta-3}{\delta-1}\right)^{1/2}\frac{(\gamma-1)}{\beta^{1/2}}\times\frac{\beta\delta^2-4\beta\delta+3\beta}{(\beta\delta^2-2\beta\delta+3\beta-\delta)^{1/2}}\ \frac{\delta-2\beta\delta+6\beta-3}{2\beta\delta^2-4\beta\delta-2\delta+6\beta}\ . \tag{106}$$

The claim[78] that $\chi^*=0$ in the linear model is clearly seen to be incorrect. For classical exponents (the mean-field case) one has instead of Eq. (102) simply

$$\chi=C_0\gamma^{-\gamma}\ . \tag{107}$$

For $\theta\to\theta^*$, i.e., $\theta\to\infty$, Eq. (89) requires $r\to 0$ and thus Eq. (107) yields a divergent susceptibility for $H\to H^*$, as found explicitly in Eq. (50).

From Eqs. (99) and (100) it is seen that various types of singular behavior at H^* are consistent with static scaling, of course. The question has to be raised if the linear model description in Eqs. (101)–(106) has a significance for real systems. In favor of the linear model we mention: (i) It holds in the limiting mean-field case, and to leading order in the $\epsilon_d=4-d$ expansion for the Ising model[79]; (ii) it is consistent with existing series-expansion analysis for the three-dimensional Ising model[80]; (iii) it is consistent with the experimental data on $CrBr_3$ and He.[77] In contrast we mention (i) small but significant deviations have been found in series analysis of the two-dimensional Ising model[80]; (ii) small but significant deviations have been found in experiments on several other substances.[78] Nevertheless we evaluated it numerically to compare it to the two-dimensional Ising simulation results in Fig. 21(a), and note striking agreement. The theoretical coercive fields are very close to the experimental values found from the dynamic condition of sufficient "flatness" of the $\phi(t)$ curve, i.e.,

$$\tau_R\approx 10^2\,\tau_{\delta\mu\delta\mu}\ . \tag{108}$$

The spinodal curve estimated by Gaunt and Baker[6] is also shown in the figure and is less consistent with our data. If their spinodal singularity exists it can have only an extremely tiny effect on the magnetization curve, since the amplitude of $\langle\mu\rangle^*$ and B differs only by about 1%, so that it is hardly detected by any experimental procedure. Perhaps the smallness of the effect and the large error estimate given are an indication that the singularity is weaker than spinodal; additional series analysis would be useful to clarify that point.

The slight discrepancies between the absolute values of the magnetization and the theoretical prediction are due to correction terms to scaling, as can be seen in the case $H=0$ where the exact solution is available.[59] These correction terms are important since our data do not strictly belong to the "critical region" if it is defined by the simultaneous conditions

$$|\epsilon|\ll 1,\quad\left|\frac{\mu_B H}{k_B T}\right|\ll 1,\quad|\langle\mu\rangle|\ll 1\ , \tag{109}$$

since the last of these conditions is violated. Nevertheless it is to be expected that the qualitative features found so far are also valid outside of the critical region.

In the other part of the figure we compare the data to Eq. (A22). Again excellent agreement is found; the main disadvantage of this description is, however, that it extends to unreasonably high values of $-\mu_B H/k_B T$.

Being interested in the behavior of the three-dimensional world we give also the three-dimensional counterpart of Fig. 21 for the bcc lattice in

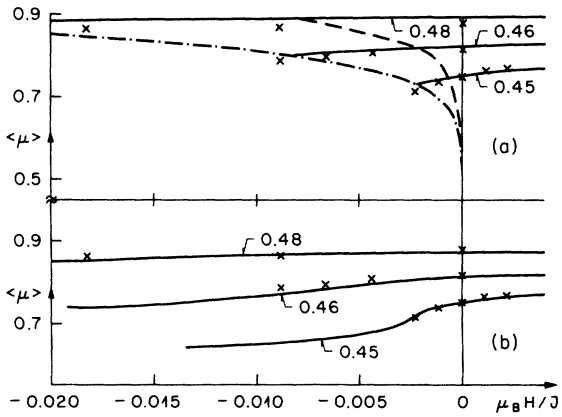

FIG. 21. Magnetization of metastable states $\langle\mu\rangle$ plotted vs the field for $d=2$. (a) Full curves are the linear model prediction and (b) cluster model prediction [Eq. (A22)]. The dash-dot curve is the linear model prediction of the magnetization $\langle\mu\rangle^*$ at the coercive field [Eq. (104)], the dashed curve shows $\langle\mu\rangle^*$ at the "pseudospinodal" predicted in Ref. 6. Parameter of the curves is J/k_BT. The symbols (×) denote the simulation results for $N=110$.

Fig. 22. Here no numerical Monte Carlo work was performed, but both Eqs. (A22) and (89), (93), and (101) have been evaluated. Note that there is nearly a coincidence of the position of the coercive fields predicted by the linear model equation of state and the series extrapolation,[6] and only the nature of the singularity there is uncertain. We conclude suggesting that the linear model prediction of H^* [Eq. (103)] should be quite reliable for all those experimental cases where it is found to describe the equilibrium properties satisfactorily.[77] In any case the possibility must be considered that H^* cannot be reached experimentally because of heterogeneous nucleation processes at defects, surfaces, etc.,[81] thus probably the question of the singularity at H^* is a purely academic one.

Finally, we mention what happens if we extend the extrapolation to fields $-H$ exceeding $-H^*$. Here both θ and $\langle\mu\rangle$ are complex, and it is found for the imaginary part of $\langle\mu\rangle$ in the linear model:

$$\begin{aligned} &\mathrm{Im}\langle\mu\rangle \propto (H^* - H)^{1/2} \quad \text{(classical case)}, \\ &\mathrm{Im}\langle\mu\rangle \propto (H^* - H)^{3/2} \quad \text{(nonclassical case)}. \end{aligned} \tag{110}$$

Sometimes the imaginary part is associated with the inverse lifetime of the metastable state.[4,8] In any case we may take Eqs. (110) as an indication that states with $-H$ exceeding $-H^*$ are unstable.

V. CONCLUSIONS

Considering the question of the nature and properties of metastable states we adopted a heuristic point of view. *First*, we considered a very simple model, the two-dimensional kinetic Ising model,[11] with a single-spin-flip transition probability. The advantages of this model are that (i) several static equilibrium properties are known exactly[59]; (ii) most equilibrium properties can be understood by means of an intuitively appealing cluster description[5]; (iii) the dynamics of the fluctuations around the equilibrium state can be investigated by high-temperature[54] and Wilson[65] expansion techniques, and, most important in our context, (iv) it is very suitable for a treatment by the Monte Carlo computer-simulation technique.[14] In fact, the reliability of this method was crucially tested recalculating several properties numerically in cases where the exact answer was available,[22,82,83] and subsequently it was used to provide rather direct numerical evidence for the cluster description,[60,61] and to calculate the time-displaced correlation functions[18] and their critical slowing down[22] in the equilibrium states. Thus it was a natural generalization of techniques developed systematically in previous investigations, to treat the nonequilibrium relaxation phenomena associated with a sudden reversal of the magnetic field. *Second*, we used a criterion to construct the metastable states, which is both simple and adequate to numerical work. It is based on the characteristics of a dynamic process, namely, the property of "sufficient flatness" [Eq. (108)] of a nonequilibrium relaxation function [Eqs. (9) and (13)–(16)]. While the criterion certainly meets "first-principle" requirements,[4] it is only a necessary criterion and perhaps not a sufficient one: it might well lead to the inclusion of states which are very slowly varying in time but not "really metastable." However, to our mind the meaning of "really metastable" is by no means clear. Thus we disregard any possible restriction of our criterion—which could readily be added *if and only if* some knowledge about the nature of metastable states were available—and include all the states found by our flatness procedure. In practice we consider all states as being metastable if their relaxation time τ_R [Eq. (16)] considerably exceeds the relaxation time of the corresponding equilibrium state $\tau_{\delta\mu\delta\mu}$ [Eq. (33)], i.e., $\tau_R \gtrsim 10^2 \times \tau_{\delta\mu\delta\mu}$. If we took 10^3 instead of 10^2, this would change the location of the "limit of metastability"

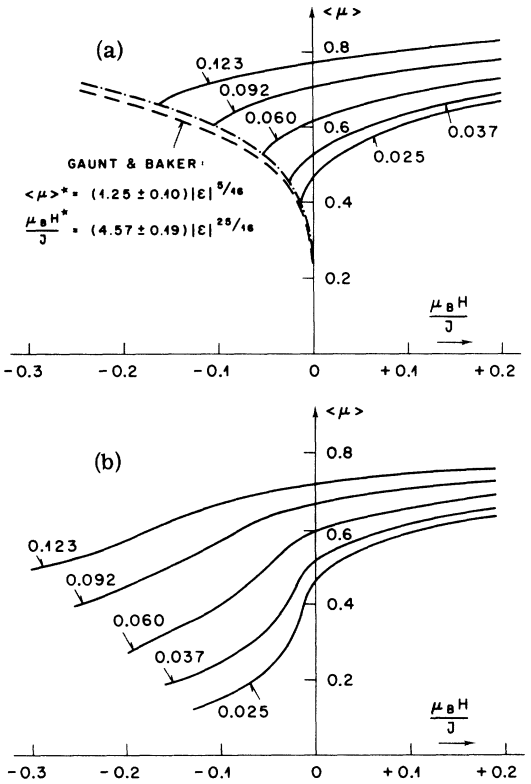

FIG. 22. Magnetization of metastable states $\langle\mu\rangle$ plotted vs the field for the $d=3$ bcc lattice. (a) Full curves are the linear model prediction and (b) cluster model prediction [Eq. (A22)]. The dash-dot curve is the linear model prediction of the magnetization $\langle\mu\rangle^*$ at the coercive field [Eq. (103).] The dashed curve shows $\langle\mu\rangle^*$ at the "pseudospinodal" predicted in Ref. 6. Parameter of the curves is ϵ.

(is equal to "coercive field") by probably only several percent.

The heuristic procedures outlined so far lead to the following results:

(i) The kinetic Ising model exhibits well-defined (i.e., reproducible) metastable states smoothly joining the stable states at $H = 0$. In the numerical work no singular behavior at $H = 0$ could be detected, as expected. Neither does the order parameter of these states depend on the size of the system N if periodic boundary conditions are used, nor does the position of the coercive field H^* (which is not precisely sharply defined, however, as indicated above). We do not find the least indication of any singular behavior in the $\langle \mu \rangle$-vs-H curves as necessary for the existence of a spinodal; however, numerical series extrapolations[6] predicting the existence of a spinodal also predict an extremely tiny effect of this singularity, since the range of H values where χ is large is extremely small; thus it must be overlooked in any kind of experimental work, and consequently our results cannot rule out the existence of a spinodal. On the contrary, our results confirm the prediction that a broad mean-field-like "spinodal region" (i.e., values of H where χ is large) does not exist in the Ising model.

(ii) It is shown that the metastable states satisfy the static scaling hypothesis, as do the (stable) equilibrium states. Moreover, also the nonequilibrium relaxation function satisfies the dynamic scaling hypothesis, as do the equilibrium relaxation functions. While these hypotheses rest on numerical evidence in our case only, they are exact in the exactly soluble mean-field case.[4] In order to exploit the scaling behavior of the metastable state, we discussed the scaling equation of state in terms of the Schofield parametric representation[76] in some detail. It is shown that this theory suggests the existence of some coercive field H^*, but is consistent with singularities which may be spinodal as well as weaker than spinodal. The latter possibility applies if one takes the "linear model equation of state",[77] which is shown to be a surprisingly good representation of our data. The coercive fields predicted nearly coincide with the ones found from our dynamic requirement. On the other hand, the coercive fields predicted by the series extrapolation are considerably smaller.[6] Since the error limits given are very large,[6] however, further series work would be very useful to eliminate this discrepancy. In three dimensions the more accurate series extrapolation results for H^* nearly coincide with the linear model prediction (although the predicted singularities, there, are different!).

(iii) The complete simulation technique was feasible to yield a detailed description of the nucleation process. Apart from the "raw-data" configurations where the growth of critical clusters, etc., could be observed,[21] the time-dependent cluster distribution $n'_s(t)$ was obtained with reasonable accuracy. In order to elucidate the consequences of these numerical results we gave a new derivation of the nucleation theory[28] appropriate to the kinetic Ising model. The various nucleation equations[28,41] previously conjectured appeared to be very crude approximations to an exact reformulation of the master equation. The nucleation theory was constructed in consistency with static scaling by use of Fisher's cluster model[5] which was discussed in the Appendix; consistency with dynamic scaling was introduced in a more *ad hoc* fashion, since too little knowledge about cluster-cluster interactions is available. Variation of the relaxation time with the magnetic field is consistent with the computer experiment. More detailed information about the cluster distribution $n'_s(t)$ has been obtained by numerical integration in the simplest case only, namely, the linearized conventional nucleation theory[41] (where clusters grow and shrink in steps of single spins only). It is seen that this theory cannot account for the actual behavior, as expected. Since too many unknown parameters are involved, no numerical solution of the more complicated nucleation equations has been attempted. Rather it was the aim of the present approach, to elucidate the various crude approximations involved in such a theory. It is suggested that the detailed properties of cluster-cluster reactions be investigated in future work along these lines.

(iv) It was shown that a simple continuation of the cluster model to negative fields [Eq. (A22)] can account for the numerical data very closely, apart from the fact that it does not yield the location of the coercive field. This formula is numerically very close to the linear model prediction both in two and in three dimensions. This good agreement leads to the conjecture that both approaches could be used to predict the order parameter of the metastable states of physical systems with reasonable confidence. Note that both the linear model[71] and the cluster model[84] have been used successfully for the representation of experimental data of equilibrium states. Thus accurate experimental information about the metastable states in the critical region would be very useful to perform a crucial test of the hypotheses proposed in our treatment which goes beyond the kinetic Ising model. One experiment of the type suggested is available for He^3 [92]; while the general trends agreed with the linear model description quite well, in one case a larger value for the limit of metastability was found. Further research along similar lines seems highly desirable, since on the macroscopic scale the lifetime of the metastable phase is perhaps also determined by the ve-

locity of interface motion; the macroscopic separation of stable and metastable phases and the completion of an interface in gas-liquid systems are due to gravitational effects, not considered in our lattice gas investigation. With respect to the theoretical approach, further numerical research seems possible concerning the details of cluster-cluster interactions. Unfortunately, the most interesting questions of the analytic behavior at the coexistence curve and at the limit of metastability are inaccessible by the present techniques.

ACKNOWLEDGMENTS

For valuable discussions and comments we are grateful to P.C. Hohenberg, P.F. Meier, T. Schneider, and D. Stauffer. We thank E. Stoll for discussions and comments and express our gratitude to him for putting at our disposal his Monte Carlo and cluster-counting programs with which parts of the Monte Carlo calculations were made.

APPENDIX: FISHER CLUSTER MODEL

By a cluster one denotes a group of reversed spins linked together by nearest-neighbor bonds. The thermal equilibrium concentration n_l of clusters with l spins is approximated by[5,25-27] [$\epsilon = 1 - T/T_c$]

$$n_l \underset{l\to\infty}{\approx} e^{-f_l/k_BT} \approx q_0 l^{-\tau} \exp\left(-a\frac{J}{k_BT}\epsilon l^{\sigma} - \frac{2H\mu_B}{k_BT} l\right) \quad . \tag{A1}$$

Here the free energy f_l of the cluster is approximated by a "bulk" term ($\propto l$) and a "surface" term ($\propto l^{\sigma}$), as discussed in Sec. III B, and a logarithmic correction term $\tau \ln l$ is also added. The constants q_0, a, τ, and σ are related to critical exponents and amplitudes.[5,25-27,85] For the sake of clarity we recall these relations. The magnetization is given by

$$\langle \mu \rangle = 1 - 2\sum_{l=1}^{\infty} l n_l \quad . \tag{A2}$$

Differentiating Eq. (A2) with respect to ϵ yields for $\epsilon \to 0$,

$$\frac{\partial \langle \mu \rangle}{\partial \epsilon} \equiv \beta B \epsilon^{\beta-1} = \frac{2q_0}{\sigma}\left(a\frac{J}{k_BT}\right)^{-(2-\tau)/\sigma} \times \Gamma\left(\frac{2+\sigma-\tau}{\sigma}\right)\epsilon^{-(2+\sigma-\tau)/\sigma} \quad , \tag{A3}$$

which yields

$$\beta = (\tau - 2)/\sigma \quad . \tag{A4}$$

Similarly, one finds differentiating Eq. (A2) with respect to the field,

$$\frac{\partial \langle \mu \rangle}{\partial H} = \frac{4q_0\mu_B}{k_BT}\sum_{l=1}^{\infty} l^{2-\tau} \exp\left(-a\frac{J}{k_BT}\epsilon l^{\sigma} - \frac{2H\mu_B}{k_BT} l\right) \quad , \tag{A5}$$

for the magnetic isotherm [$\epsilon \equiv 0$]

$$\frac{\partial \langle \mu \rangle}{\partial H} \equiv \frac{1}{\delta} D H^{1/\delta - 1} = \frac{4q_0\mu_B}{k_BT}\left(\frac{2H\mu_B}{k_BT}\right)^{\tau-3}\Gamma(3-\tau) \, , \tag{A6}$$

which implies

$$\delta = 1/(\tau - 2) \quad . \tag{A7}$$

On the other hand, Eq. (A5) yields for the susceptibility ($H = 0$, $\epsilon < 0$)

$$\left.\frac{\partial \langle \mu \rangle}{\partial H}\right|_{H=0} \equiv C^{-}\epsilon^{-\gamma} = \frac{4q_0\mu_B}{k_BT}\left(\frac{aJ}{k_BT}\right)^{-(3-\tau)/\sigma} \epsilon^{-(3-\tau)/\sigma} \times \Gamma\left(\frac{3-\tau}{\sigma}\right) \quad , \tag{A8}$$

which implies

$$\gamma = (3 - \tau)/\sigma \tag{A9}$$

and the scaling law[25-27,75]

$$\gamma = \beta(\delta - 1) \quad . \tag{A10}$$

All critical exponents α, β, γ, δ, ... are determined by two basic exponents σ and τ,

$$\tau = 2 + 1/\delta, \quad \sigma = 1/(\beta\delta) = 1/(\gamma + \beta) \quad , \tag{A11}$$

and all critical amplitudes A, B, C, D, ... are determined by *two* basic constants a and q_0 in agreement with the universality hypothesis of Betts *et al.*[86] While the exponent relations are exact in the two-dimensional Ising model, the amplitude relations hold only approximately. Kiang[87] suggested that the cluster model might be used for all l down to $l = 1$, implying a further relation for the q_0, from the condition that $\langle \mu \rangle = 0$ at T_c,

$$q_0^{-1} = 2\zeta(\tau - 1) \quad , \tag{A12}$$

where ζ is the ζ function.[88] For $d = 2$ Eq. (A12) implies $q_0 \approx 0.032$ and Eq. (A3) implies $a \approx 7.45$. Further properties of the clusters may be derived from the requirement,[89] that the typical size $\overline{V}$ of clusters leading to the divergence of the susceptibility in Eq. (A8) is the correlation volume ξ^d, where ξ is the correlation length and d is the dimensionality of the system

$$\xi \equiv \xi_0 \epsilon^{-\nu} \quad . \tag{A13}$$

From the ansatz for the volume of a cluster with l reversed spins

$$V \cong \hat{V} l^{z} \quad , \tag{A14}$$

one derives[90]

$$\overline{V} \equiv \xi_0^d \epsilon^{-\nu d} = \hat{V}\frac{\int_0^{\infty} l^{2+z-\tau} e^{-a(J/k_BT)\epsilon l^{\sigma}} dl}{\int_0^{\infty} l^{2-\tau} e^{-a(J/k_BT)\epsilon l^{\sigma}} dl} = \hat{V}\epsilon^{-z/\sigma}\left(a\frac{J}{k_BT}\right)^{-z/\sigma}\frac{\Gamma((3+z-\tau)/\sigma)}{\Gamma((3-\tau)/\sigma)} \quad , \tag{A15}$$

TABLE I. Exponents of clusters in the Ising model.

Bulk energy	Volume	Surface	Geometrical limit for surface	Surface free energy	Bulk critical exponents	Dimensionality
$\propto l^y$	$\propto l^z$	$\propto l^{\sigma'}$	$\propto l^{(1-1/d)(1+1/\delta)}$	$\propto l^{\sigma}$		
y	z	σ'	$(1-1/d)(1+1/\delta)$	σ	β,δ,γ	d
1	$\frac{16}{15}$	$\frac{3}{5}$	$\frac{8}{15}$	$\frac{8}{15}$	$\frac{1}{8}, 15, \frac{7}{4}$	2
1	$\frac{6}{5}$	$\frac{21}{25}$	$\frac{4}{5}$	$\frac{16}{25}$	$\frac{5}{16}, 5, \frac{5}{4}$	3
1	$\frac{4}{3}$	1	1	$\frac{2}{3}$	$\frac{1}{2}, 3, 1$	4

i.e., using $d\nu = \beta(\delta+1)$,

$$V_l = \hat{V} l^{1+1/\delta} \tag{A16}$$

or for the density difference $\rho_l = l/V_l$ between the clusters and the surrounding bulk

$$\rho_l = \hat{V}^{-1} l^{-1/\delta} \quad , \tag{A17}$$

which may be interpreted in terms of the fact that for large clusters the probability that they contain "bubbles"[90] is enhanced. For the mean surface of clusters with l spins it is required that

$$S_l = \hat{S} l^{\sigma'} \quad , \quad \sigma' \geq (1-1/d)(1+1/\delta) \quad . \tag{A18}$$

Now the l dependence of the surface free energy is found from

$$f_l^{\text{surf}} \propto \rho_l \, S_l \propto l^{-1/\delta} l^{\sigma'} = l^{\sigma} \quad , \tag{A19}$$

which implies[90]

$$\sigma' = \sigma + 1/\delta \quad . \tag{A20}$$

We summarize these various predictions about static cluster properties in Table I.[60,90] It is seen that the inequality [Eq. (A18)] is indeed fulfilled (it would be violated for $d=3$, 4 if one had required $\sigma' = \sigma$). These relations should hold for $l \gg 1$, but l should not be too large: If l^z exceeds the correlation volume considerably, the geometrical limit is valid.

The cluster model has the deficiencies that it is difficult to use above T_c, and that it is not symmetric with respect to a reversal of the magnetic field.[85,90,91] Since its validity seemed rather questionable, computer experiments were undertaken to check it by direct investigation of cluster.[60,61] The values for σ' of Table I have been confirmed both for $d=2$ and 3,[60] while Eq. (A1) was confirmed for $d=2$.[61] The latter investigation revealed that Eq. (A12) is not quite correct, since deviations from Eq. (41) occur for $l \leq 7$.

The aspect of the cluster model which is most important in the context of metastability is the essential singularity at $H=0$. For $H<0$, f_l has a maximum at l^*, and n_l has a minimum at l^*, where

$$l^* \approx \left(a\sigma \frac{J}{k_B T} \epsilon \frac{k_B T}{-2H\mu_B} \right)^{1/(1-\sigma)} \quad , \tag{A21}$$

and for $l > l^*$, n_l increases exponentially. This means that Eq. (A1) cannot be correct for large l in a metastable state. By computer simulation we investigated the question whether Eq. (A1) is a realistic description for intermediate l. This is shown in Fig. 23, where the cluster distribution is plotted both for $\mu_B H/k_B T = 0.000$ and $\mu_B H/k_B T = -0.003$ at $J/k_B T = 0.46$. Since for calculation of the theoretical distributions the amplitude relations Eqs. (A3) and (A12) have been used, no adjustable parameters occur. The scatter of data points for $l \geq 100$ is fully attributable to poor statistics (note the small absolute values of n_l!), so we find that Eq. (A1) holds also for metastable states for $l \gtrsim 7$, $l \ll l^*$. This observation supports the suggestion that supercritical clusters ($l > l^*$) are characteristic for the new phase with reversed magnetization, and should be removed from the sum Eq. (A2) cal-

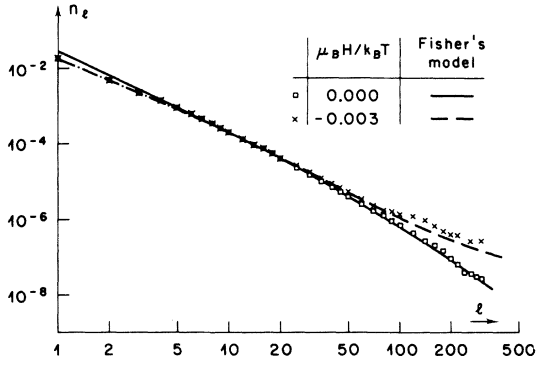

FIG. 23. Cluster distribution n_l in an equilibrium state [□] and in a metastable state [×] for $J/k_B T = 0.46$ and $N = 110$. The curves are the prediction of the cluster model [Eq. (A1)] where the constants a, q_0 are taken from Eqs. (A3) [where $B = 1.22$ (Ref. 59)] and (A12). In the metastable state shown the critical cluster size is $l^* \cong 2452$.

culating the magnetization,[8,10]

$$\langle \mu \rangle_{\mathrm{MS}} = 1 - 2 \sum_{l=1}^{l^*} l n_l \quad . \tag{A22}$$

The existence of an analytic continuation of this type is also supported by the fact that all derivatives of $\langle \mu \rangle$ with respect to H exist for $H = 0+$ in the cluster model. Equation (A22) leads to a completely smooth behavior of the magnetization as a function of the magnetic field (apart from small unphysical jumps at all integer values of l^*). This approach does not yield any definition for a coercive field, H^*, except one takes the extreme possible value $l^* = 1$ as a definition for H^*. Figure 21(b) shows that this suggestion is incorrect, it leads to values of H^* which are orders of magnitude too large. Taking $(l^*)^{1+1/\delta} = \xi^d$ as a definition of H^* is more reasonable, but the values of H^* are still one order of magnitude too large. Apart from this difficulty the numerical agreement between Eq. (A22) and the data is surprisingly good. One is led to the conclusion that H^* should be associated with the position of maximum slope in the $\langle \mu \rangle$-vs-H curve.

---

*IBM Postdoctoral Fellow from Physikdepartment E 14, Technische Universität München, 8046 Garching, W. Germany; now returned.

†Guest scientist from Physikdepartment E 14, Technische Universität München, 8046 Garching, West Germany.

[1]J. van der Waals, Thesis (Leiden, 1873) (unpublished).

[2]J. L. Lebowitz and D. Penrose, J . Math. Phys. 7, 98 (1966).

[3]O. Penrose and J. L. Lebowitz, J. Stat. Phys. 3, 211 (1971).

[4]K. Binder, Phys. Rev. B 8, 3419 (1973).

[5]M. E. Fisher, Physics 3, 255 (1967). An essential singularity at the coexistence curve was also proposed by A. F. Andreev, Zh. Eksp. Teor. Fiz. 45, 2064 (1963) [Sov. Phys.-JETP 18, 1415 (1964)].

[6]D. S. Gaunt and G. A. Baker, Phys. Rev. B1, 1184 (1970).

[7]B. Chu, F. J. Schoenes, and M. E. Fisher, Phys. Rev. 185, 219 (1969).

[8]J. S. Langer, Ann. Phys. (N. Y.) 41, 108 (1967).

[9]R. B. Griffiths, C. Y. Weng, and J. S. Langer, Phys. Rev. 149, 301 (1966).

[10]C. Domb, J. Phys. C 6, 39 (1973).

[11]R. J. Glauber, J. Math. Phys. 4, 294 (1963).

[12]M. Suzki and R. Kubo, J. Phys. Soc. Jap. 24, 51 (1968).

[13]K. Kawasaki, in *Phase Transitions and Critical Phenomena*, edited by C. Domb and M. S. Green (Academic, New York, 1972), Vol. 2, p. 443.

[14]N. Metropolis, A. W. Rosenbluth, M. N. Rosenbluth, A. H. Teller, and E. Teller, J. Chem. Phys. 21, 1987 (1953).

[15]L. D. Fosdick, in *Methods of Computational Physics*, edited by B. J. Alder (Academic, New York, 1963) Vol. 1, p. 245.

[16]K. Binder and H. Rauch, Z. Phys. 219, 201 (1969).

[17]N. Ogita, A. Ueda, T. Matsubara, H. Matsuda, and F. Yonezawa, J. Phys. Soc. Jap. 26S, 146 (1969).

[18]H. Müller-Krumbhaar and K. Binder, J. Stat. Phys. 8, 1 (1973).

[19]E. Stoll and T. Schneider, Phys. Rev. A 6, 429 (1972).

[20]A. Compagner, J. Phys. Soc. Jap. Suppl. 26, 229 (1969); Thesis (Utrecht, 1972) (unpublished).

[21]T. Schneider and E. Stoll (unpublished).

[22]E. Stoll, K. Binder, and T. Schneider, Phys. Rev. B 8, 3266 (1973).

[23]J. S. Langer, Ann. Phys. (N. Y.) 54, 258 (1969); Am. Phys. (N. Y.) 65, 53 (1971); J. S. Langer and M. Bar-on, Ann. Phys. (N. Y.) 78, 421 (1973).

[24]J. S. Langer, Phys. Rev. Lett. 27, 973 (1968); R. Landanen and J. A. Swanson, Phys. Rev. 127, 1668 (1961).

[25]M. E. Fisher, J. Appl. Phys. 38, 981 (1967).

[26]M. E. Fisher, Rep. Prog. Phys. 30, 615 (1967).

[27]M. E. Fisher, in *Proceedings of the International School of Physics "Enrico Fermi" on Critical Phenomena, Course* 51, edited by M. S. Green (Academic, New York, 1971).

[28]C. S. Kiang, D. Stauffer, G. H. Walker, O. P. Puri, J. D. Wise, Jr., and E. M. Patterson, J. Atmos. Sci. 28, 1112 (1971).

[29]A. Eggington, C. S. Kiang, D. Stauffer, and G. H. Walker, Phys. Rev. Lett. 26, 820 (1971).

[30]K. Binder and E. Stoll, Phys. Rev. Lett. 31, 47 (1973).

[31]J. W. Gibbs, *Collected Works* (Longman Green, New York, 1931).

[32]P. Glansdorff and I. Prigogine, *Thermodynamic Theory of Structure, Stability and Fluctuations* (Wiley, New York, 1971).

[33]If the lattice gas version (Refs. 26 and 27) of the Ising model is preferred, one has to interpret H as a chemical potential.

[34]Ref. 32, p. 58.

[35]R. Becker and W. Döring, Ann. Phys. (Leipz.) 24, 719 (1935).

[36]M. Volmer and A. Weber, Z. Phys. Chem. 119, 277 (1926).

[37]W. A. Johnson and R. F. Mehl, Trans. AIME. 135, 416 (1939).

[38]J. E. Burke and D. Turnbull, Prog. Met. Phys. 3, 222 (1952).

[39]J. Frenkel, *Kinetic Theory of Liquids* (Dover, New York, 1955).

[40]M. E. Fine, *Introduction to Phase Transformations in Condensed Systems* (Academic, New York, 1964).

[41]J. Feder, K. C. Russell, J. Lothe, and G. M. Pound, Adv. Phys. 15, 117 (1966).

[42]Nucleation theory in its conventional form (Refs. 34–40) was used for the Ising model by G. Adam in Refs. 43 and 44.

[43]G. Adam, Z. Naturforsch. B 23, 181 (1968).

[44]G. Adam, Z. Phys. Chem. 68, 113 (1968).

[45]For general introductions about these techniques see Refs. 26 and 46.

[46]C. Domb, Adv. Phys. 9, 149 (1960); Adv. Phys. 19, 339 (1970).

[47]D. E. Lanford and D. Ruelle, Commun. Math. Phys. 13, 194 (1969).

[48]J. W. Cahn, Acta Mettall. 9, 795 (1961); Acta Mettall. 10, 179 (1962).

[49]J. W. Cahn and J. E. Hilliard, J. Chem. Phys. 28, 258 (1958).

[50]N. N. Bogoliubov, in *Studies in Statistical Mechanics*, edited by J. de Boer and G. E. Uhlenbeck (North-Holland, Amsterdam, 1962).
[51]We denote by H' the magnetic field of the initial state of the nonequilibrium process, and by H the field of the final state.
[52]The magnitudes of the changes may depend on the lattice site l.
[53]M. Suzuki, Int. J. Magn. 1, 123 (1971).
[54]H. Yahata and M. Suzuki, J. Phys. Soc. Jap. 27, 1421 (1969); H. Yahata, J. Phys. Soc. Jap. 30, 657 (1971).
[55]D. Bedeaux, K. E. Shuler, and I. Oppenheim, J. Stat. Phys. 2, 1 (1970).
[56]More complete references on various applications are given in Ref. 18.
[57]A detailed qualitative description of this process is also given in Ref. 21.
[58]L. Onsager, Phys. Rev. 65, 117 (1944).
[59]C. N. Yang, Phys. Rev. 85, 809 (1952).
[60]K. Binder and D. Stauffer, J. Stat. Phys. 6, 49 (1972).
[61]E. Stoll, K. Binder, and T. Schneider, Rev. Phys. B 6, 2777 (1972).
[62]D. Stauffer and C. S. Kiang, Phys. Rev. Lett. 27, 1783 (1971).
[63]R. A. Ferrell, N. Menyhard, H. Schmidt, F. Schwabl, and P. Szepfalusy, Ann. Phys. (N.Y.) 47, 565 (1968); Phys. Rev. Lett. 18, 891 (1967).
[64]B. I. Halperin and P. C. Hohenberg, Phys. Rev. 177, 952 (1969); Phys. Rev. Lett. 19, 700 (1967).
[65]B. I. Halperin, P. C. Hohenberg, and S. K. Ma, Phys. Rev. Lett. 29, 1548 (1972).
[66]For a more detailed discussion of the stability of these solutions see Refs. 4 and 9.
[67]R. Brout, *Phase Transitions* (Benjamin, New York, 1965).
[68]G. Adam, in *Proceedings of the International Symposium on Synergetics*, edited by H. Haken (Teuber, Stuttgart, 1973), p. 220.
[69]J. L. Katz, H. Saltsburg, and H. Reiss, J. Colloid Interface Sc. 21, 560 (1966).
[70]D. Stauffer, C. S. Kiang, A. Eggington, E. M. Patterson, O. P. Puri, G. H. Walker, and J. D. Wise, Jr., Chem. Phys. Lett. 16, 499 (1972).
[71]K. W. Sarkies and N. E. Frankel, J. Chem. Phys. 54, 433 (1971); see also J. S. Langer and J. Turski (unpublished).
[72]F. F. Abraham, J. Chem. Phys. 51, 1632 (1969).
[73]A numerical solution of Eq. (62b) is mentioned in Ref. 28.
[74]Continuous System Modeling Program III (CSMPIII), Program Reference Manual, IBM Corp., Data Processing Div., 1133 Westchester Avenue, White Plains, N.Y., 1972.
[75]R. B. Griffiths, Phys. Rev. 158, 176 (1967); B. Widom, J. Chem. Phys. 43, 3898 (1965).
[76]P. Schofield, Phys. Rev. Lett. 22, 606 (1969).
[77]P. Schofield, J. D. Litster, and J. T. Ho, Phys. Rev. Lett. 23, 1098 (1969); J. T. Ho and J. D. Litster, Phys. Rev. B 2, 4523 (1970).
[78]M. Vicentini-Missioni, in Ref. 13.
[79]E. Brezin, D. T. Wallace, and K. G. Wilson, Phys. Rev. Lett. 29, 591 (1972).
[80]C. Domb and D. S. Gaunt, J. Phys. C 3, 1442 (1970).
[81]D. Stauffer, C. S. Kiang, A. Eggington, E. M. Patterson, O. P. Puri, G. H. Walker, and J. D. Wise, Jr., Phys. Rev. B 6, 2780 (1972).
[82]R. Friedberg and J. E. Cameron, J. Chem. Phys. 52, 6049 (1970).
[83]K. Binder, Physica 62, 508 (1972).
[84]W. Rathjen, D. Stauffer, and C. S. Kiang, Phys. Lett. A 40, 345 (1972).
[85]C. S. Kiang and D. Stauffer, Z. Phys. 235, 130 (1970).
[86]D. D. Betts, A. J. Guttmann, and G. S. Joyce, J. Phys. Chem. C 4, 1994 (1971).
[87]C. S. Kiang, Phys. Rev. Lett. 24, 47 (1970).
[88]M. Abramovicz and I. Stegun, *Handbook of Mathematical Functions* (Dover, New York, 1967).
[89]L. P. Kadanoff, in Ref. 27.
[90]D. Stauffer, C. S. Kiang, and G. H. Walker, J. Stat. Phys. 3, 323 (1971).
[91]L. Reatto, Phys. Lett. A 33, 519 (1970); Phys. Rev. B 5, 204 (1972).
[92]D. Dahl and M. R. Moldover, Phys. Rev. Lett. 27, 1421 (1971).